https://doi.org/10.15407/ufm.26.03.461

S.P. REPETSKY 1,2,*, I.G. VYSHYVANA 3,**, V.V. LIZUNOV 1,***, R.M. MELNYK 2, M.I. REZNIKOV 3, T.M. RADCHENKO 1, and V.A. TATARENKO 1

- ¹G.V. Kurdyumov Institute for Metal Physics of the N.A.S. of Ukraine, 36 Academician Vernadsky Blvd., UA-03142 Kyiv, Ukraine
- ² National University of Kyiv-Mohyla Academy,
- 2 H. Skovoroda Str., UA-04070 Kyiv, Ukraine
- ³ Taras Shevchenko National University of Kyiv, 60 Volodymyrs' ka Str., UA-01033 Kyiv, Ukraine
- * srepetsky0208@gmail.com, ** i.vyshyvana@gmail.com, *** lizunov.vvacheslav@gmail.com

GREEN'S FUNCTION TECHNIQUE IN THE THEORY OF DISORDERED CRYSTALS: APPLICATION TO POTASSIUM-DOPED GRAPHENE

The method of describing the energy spectrum, free energy, and electrical conductivity of disordered crystals based on the use of the Hamiltonian of electrons and phonons is reviewed, analysed, and developed. The electron states of a system are described through the tight-binding model. A simple procedure for calculating the matrix elements of the Hamiltonian within the Wannier's representation is proposed. Expressions for the Green's functions, free energy, and electrical conductivity are derived using the diagram method. Using this procedure, the vertex parts of the mass operators of the electron-electron and electron-phonon interactions are renormalized. A set of exact equations is obtained for the spectrum of elementary excitations in a crystal. This enables the performance of numerical calculations on the energy spectrum and the prediction of system properties with predetermined accuracy. Expressions are obtained for the static waves of concentrations, charge and spin densities, which determine the phase state of a disordered crystal. In contrast to other approaches, which account for electron correlations only within the limiting cases of infinitely large and

Citation: S.P. Repetsky, I.G. Vyshyvana, V.V. Lizunov, R.M. Melnyk, M.I. Reznikov, T.M. Radchenko, and V.A. Tatarenko, Green's Function Technique in the Theory of Disordered Crystals: Application to Potassium-Doped Graphene, *Progress in Physics of Metals*, 26, No. 3: 461–497 (2025)

© Publisher PH "Akademperiodyka" of the NAS of Ukraine, 2025. This is an open access article under the CC BY-ND license (https://creativecommons.org/licenses/by-nd/4.0)

infinitesimal electron densities, this method describes electron correlations in the general case of an arbitrary density. In addition to the theory, the results of a numerical calculation of the energy spectrum of a graphene layer with adsorbed potassium (K) atoms are presented. As established, at the K-atoms' concentration such that the unit cell includes two carbon (C) atoms and one K atom, the latter being located (adsorbed) on the graphene layer surface 0.286 nm above the C atom, the energy gap is $\cong 0.25$ eV. The location of the Fermi level (ε_F) in the energy spectrum depends on the potassium-atoms' concentration and is in the energy interval -0.36 Ry $\leq \varepsilon_F \leq -0.23$ Ry.

Keywords: disordered crystals, electronic structure, conductivity, Green's functions, the mass operator, density of states, free energy.

1. Introduction

Advances in the description of the influence of impurities on the properties of crystals are mainly due to the development of the electron theory. Traditional ideas about the effect of impurities on the properties of alloys are based on the pseudopotential construction [1] and perturbation theory. However, this theory is inapplicable in the case of a large value of the scattering potential, which takes place, for example, in alloys of simple and transition elements. In addition, due to the non-local nature of the pseudopotential, there is a problem of 'portability' of the pseudopotential. It is impossible to use nuclear potentials determined by the properties of some systems to describe other systems. The use of the theory of Vanderbilt ultrasoft potentials [2, 3] and the method of projector-augmented waves proposed by Blöchl [4, 5] allowed for achieving fundamental progress in investigating the electronic structure and the properties of the system. This approach was further developed using the generalized gradient approximation proposed in Refs. [6–10].

It should be noted that, in articles [11–17], the description of the crystals' electronic structure was carried out, including the Coulomb long-range interaction between electrons of different sites in the crystal lattice, thanks to a method based on the tight-binding model [18, 19] and the density functional theory. However, such methods are suitable only for describing the crystals characterized by ideal ordering. In disordered crystals, effects associated with localized electron states occur. These effects cannot be described within the model, where the crystal is treated as an ideal one.

In Ref. [20], a virtual crystal approximation was proposed to study the properties of alloys by the density functional theory. This approach is applied in the Vanderbilt ultrasoft pseudopotential scheme to predict the properties of $Pb(Zr_{0.5}Ti_{0.5})O_3$ solutions in their paraelectric and ferroelectric phases.

The use of the multiple-scattering theory allowed for achieving fundamental progress in investigating the electronic structure and the properties of disordered systems. The theory of the electronic structure of an al-

loy was developed in Refs. [21–25] based on the self-consistent method of Korringa-Kohn-Rostoker as the coherent potential approximation. This theory makes it possible to take into account both the change in the lifetime of elementary excitations (electrons and phonons) and the change in their energy spectrum along with the impurity concentration.

The theory of the electronic spectrum and electrical conductivity of disordered crystals was developed in Refs. [26–29] is based on the tight-binding model, the multiple-scattering theory, and the one-electron approximation. This theory takes into account both the change in the lifetime of elementary excitations (electrons and phonons) and the change in their energy spectrum with a change in the impurity concentration and degree of impurity ordering.

Articles [30–36] present a method of describing the energy spectrum, free energy, and electrical conductivity of disordered crystals based on the Hamiltonian of electrons and phonons. In papers [30–36], authors went beyond the framework of the one-electron approximation. Electron states of a system are described by the tight-binding model. Calculations of two-time Green's functions are based on the temperature Green's functions. These use a known relation between the spectral representation of the two-time and temperature Green's functions. The calculation of the temperature Green's functions for a disordered crystal is based on diagram techniques, which is a generalization of the diagram technique for homogeneous systems [37]. A set of exact equations is obtained for the spectrum of elementary excitations in a crystal. This makes it possible to perform numerical calculations of the energy spectrum and to predict the properties of the system with a predetermined accuracy.

Most theoretical studies of the energy spectrum of graphene are based on the density functional theory. The most significant achievements relate to the self-consistent meta-generalized gradient approximation within the projector-augmented-wave method [10], which is implemented within the VASP and Quantum ESPRESSO software packages. Numerical calculations performed by this method show the opening of the gap in the energy spectrum of graphene due to the presence of impurities. However, to determine the nature of the effect of impurities on the energy spectrum and the properties of graphene, it is not enough to limit the numerical calculations performed by the above methods. It is clear that, to determine the nature of the gap in the energy spectrum of graphene, a quantitative investigation must be supported by a simple and adequate model that allows accurate analytical solutions.

In articles [26–29] in the tight-binding one-electron model, which allows accurate analytical solutions, it was first assumed that, when ordering the substitutional impurity atoms, in the energy spectrum of graphene, there is a gap, whose width depends on the order parameter and impurity potential scattering.

In this work, we present a new method of describing the electronic spectrum and electrical conductivity of graphene based on the Hamiltonian of electrons and phonons [30–36].

2. Hamiltonian of the Electron–Phonon System in a Disordered Crystal

The Hamiltonian of the disordered metallic alloy, disordered semiconductor, or disordered dielectric consists of the sum of the Hamiltonian of electrons in the nuclei field, the Hamiltonian of electron-electron interactions, and the Hamiltonian of the nuclei. Within the Wannier's representation, the system Hamiltonian is as follows [30]:

$$H = H_0 + H_{\rm int}, \tag{1}$$

where the zero-order Hamiltonian

$$H_0 = H_e^{(0)} + H_{\rm ph}^{(0)} \tag{2}$$

consists of the Hamiltonian of the electrons in the field of the cores of atoms within the perfectly ordered crystal

$$H_{e}^{(0)} = \sum_{\substack{ni\gamma\\n'i'\gamma'}} h_{ni\gamma,n'i'\gamma'}^{(0)} a_{ni\gamma}^{\dagger} a_{n'i'\gamma'}$$
(3)

and the harmonic phonon Hamiltonian for the motion of the cores of atoms within the ideal ordered crystal

$$H_{\rm ph}^{(0)} = \sum_{ni\alpha} \frac{P_{ni\alpha}^2}{2M_i} + \frac{1}{2} \sum_{\substack{ni\alpha\\n'i'\alpha'}} \Phi_{ni\alpha,n'i'\alpha'}^{(0)} u_{ni\alpha} u_{n'i'\alpha'}. \tag{4}$$

Symbol n is the number of a unit cell, i is the site number in a primitive unit cell, and γ denotes all other quantum numbers, including the orbital and spin ones. The symbol $h^{(0)}$ denotes the 'hopping integral' that connects the respective orbitals. For the phonon Hamiltonian, α is a spatial direction coordinate (x, y, or z), P_{nia} is the ion core momentum, M_i is the mass of the ion core, u_{nia} is the deviation of the ion core from the equilibrium site position in the lattice, and $\Phi_{nia,n'i'a'}^{(0)}$ is the corresponding spring-constants matrix.

The interaction Hamiltonian in Eq. (1) is the perturbation of the system due to all effects we will include; it is composed of 5 terms:

$$H_{\rm int} = H_{\rm ec} + H_{\rm enh} + H_{\rm ee} + H_{\rm phc} + H_{\rm phph}$$
 (5)

The electrons' Hamiltonian is modified by the term

$$H_{\text{ec}} = \sum_{\substack{ni\gamma\\n'i'\gamma'}} w_{ni\gamma,n'i'\gamma'} a_{ni\gamma}^{\dagger} a_{n'i'\gamma'}, \qquad (6)$$

which is the difference between the Hamiltonian of the electrons in the field of the cores of atoms in a disordered crystal and the Hamiltonian of the electrons in the field of the cores of atoms in a perfect ordered crystal.

The electron-phonon-interaction Hamiltonian is given by

$$H_{\text{eph}} = \sum_{\substack{ni\gamma \\ n'i'\gamma' \\ n''i'\gamma'' \\ n''i'\gamma''}} v_{n''i'\gamma'}^{\prime n''i'\gamma'} u_{n''i'\gamma'}^{\prime a_{ni\gamma}} a_{ni\gamma}^{+} a_{n'i'\gamma'}^{-}. \tag{7}$$

It will be described in more detail below.

The Hamiltonian of the Coulomb interaction between electrons is given by the term

$$H_{ee} = \frac{1}{2} \sum_{\substack{n_1, n_2, \\ n_3, n_4}} v_{n_3, n_4}^{n_1, n_2} a_{n_1}^+ a_{n_2}^+ a_{n_3}^- a_{n_4}, n = (ni\gamma).$$
 (8)

The modification of the interaction of the phonons with the ion cores caused by the disordering of the atoms is given by

$$H_{\text{phc}} = \frac{1}{2} \sum_{\substack{n \mid \alpha \\ n' i' \alpha'}} \Delta M_{n \mid \alpha, n' i' \alpha'}^{-1} P_{n \mid \alpha} P_{n' i' \alpha'} + \frac{1}{2} \sum_{\substack{n \mid \alpha \\ n' i' \alpha'}} \Delta \Phi_{n \mid \alpha, n' i' \alpha'} u_{n \mid \alpha} u_{n' i' \alpha'}, \tag{9}$$

where

$$\Delta M_{ni\alpha,n'i'\alpha'}^{-1} = \left(\frac{1}{M_{ni}} - \frac{1}{M_{i}}\right) \delta_{nn'} \delta_{ii'} \delta_{\alpha\alpha'}, \quad \Delta \Phi_{ni\alpha,n'i'\alpha'} = \Phi_{ni\alpha,n'i'\alpha'} - \Phi_{ni\alpha,n'i'\alpha'}^{(0)}, \quad (10)$$

and M_{ni} , M_i are the masses of the atoms at the site (ni) for ordered alloy and disordered one, respectively.

We also include the cubic anharmonic-potential terms for the phonons (under the assumption that they remain small and can be treated as perturbing operators):

$$H_{\text{phph}} = \frac{1}{3!} \sum_{\substack{ni\alpha \\ n'i'\alpha' \\ n''i'\alpha''}} \Phi_{ni\alpha,n'i'\alpha',n''i'\alpha''}^{(0)} u_{ni\alpha} u_{n'i'\alpha'} u_{n'i'\alpha''} u_{n''i'\alpha''}. \tag{11}$$

The values $a_{ni\gamma}^+$, a_{nig} are the operators of creation and destruction of electrons, respectively, in the state described by the Wannier's function $\phi_{ni\gamma}(\xi)$, where $\xi=(\mathbf{r},\sigma')$ are the spatial and spin coordinates of the wave function. In the second quantization representation, the set of functions $\phi_{ni\gamma}(\xi)$ represents a complete basis of orthogonal and normalized wave functions of one electron.

Wannier's functions $\phi_{ni\gamma}(\mathbf{r}, \sigma')$, on which the Hamiltonian of the system is represented as in Eq. (1), are defined by a formula

$$\phi_{ni\gamma}(\mathbf{r},\sigma') = \tilde{\psi}_{ni\delta}(\mathbf{r} - \mathbf{r}_{ni})\chi_{\sigma}(\sigma'), \qquad (12)$$

where spin part of wave function, $\chi_s(\sigma') = \delta_{\sigma\sigma'}$, is an eigenfunction z-component of the electron spin operator, $\delta_{\sigma\sigma'}$ is a Kronecker's symbol, $\gamma \equiv (\delta\sigma)$ (the state index γ is defined by the energy-band number and the projection of the spin onto the Oz axis). To construct the Wannier's functions, we use analytical expressions for the wave functions of an electron in the field of an atomic nucleus of the λ sort localized at the lattice site (ni) of

an ideally ordered crystal:

$$\Psi_{ni\delta}(\mathbf{r} - \mathbf{r}_{ni}) = R_{\tilde{\epsilon}l}(|\mathbf{r} - \mathbf{r}_{ni}|)Y_{lm}(\mathbf{r} - \mathbf{r}_{ni}), Y_{lm}(\mathbf{r} - \mathbf{r}_{ni}) = Y_{lm}(\theta, \varphi), \qquad (13)$$

where θ , φ are the angular spherical coordinates of the vector $\mathbf{r} - \mathbf{r}_{ni}$. Above-mentioned index $\delta = \tilde{\epsilon} l m$ incorporates the quantum numbers for the energy value $\tilde{\epsilon}$, the angular-momentum quantum numbers l and m, \mathbf{r} is the electron position vector, \mathbf{r}_{in} is the position vector for the atomic nuclei at the site (ni) in equilibrium:

$$\mathbf{r}_{ni} = \mathbf{r}_n + \mathbf{\rho}_i, \ \mathbf{r}_n = \sum_{\mathbf{r}} l_{\mathbf{r}} \mathbf{a}_{\mathbf{r}}; \tag{14}$$

 \mathbf{r}_n is the position vector of the *n*-th unit cell in the crystal lattice, \mathbf{a}_{v} are the main translation vectors of the crystal lattice, ρ_i is the vector of the relative position of the site of the sublattice i in the unit cell n. The coordinates $\{l_{v}\}$ of the radius vector \mathbf{r}_n of the unit cell n in the lattice are integers. The number v takes on values v=1,2,3 for three-dimensional (3D) crystals, v=1,2 for two-dimensional (2D) crystals, and v=1 for one-dimensional (1D) crystals.

Basis orthogonalization is performed with the Löwdin method [38]. The orthogonalized wave function can be represented as:

$$\tilde{\Psi}_{n_1 i_1 \delta_1}(r_1, \theta_1, \varphi_1) = \sum_{n_2 i_2 \delta_2} S_{n_2 i_2 \delta_2, n_1 i_1 \delta_1}^{-1/2} \Psi_{n_2 i_2 \delta_2}(r_2, \theta_2, \varphi_2),
\Psi_{n_2 i_2 \delta_2}(r_2, \theta_2, \varphi_2) = R_{\tilde{\epsilon}_2 l_2}(r_2) Y_{l_2 m_2}(\theta_2, \varphi_2),$$
(15)

where $S_{n_2i_2\delta_2,n_1i_1\delta_1}$ is the overlap matrix.

The matrix $S_{n_2 l_2 \delta_2, n_1 l_1 \delta_1}$ has an infinite rank. The Fourier component of the overlap matrix has a finite rank. In this regard, the Fourier component of the overlap matrix is found as follows:

$$S_{i_1\delta_1,i_2\delta_2}(\mathbf{k}) = \sum_{n_2} S_{n_1i_1\delta_1,n_2i_2\delta_2} \exp(i\mathbf{k} \cdot (\mathbf{r}_{n_2i_2} - \mathbf{r}_{n_1i_1})).$$
 (16)

The vector \mathbf{k} is defined by the expression

$$\mathbf{k} = \sum_{\mathbf{v}} k_{\mathbf{v}} \mathbf{b}_{\mathbf{v}},\tag{17}$$

where \mathbf{b}_{v} are basis vectors of translations in the reciprocal lattice; $(\mathbf{a}_{v}\cdot\mathbf{b}_{v'})=2\pi\delta_{vv'}$. In the right-hand side of formula (16),

$$\mathbf{k} \cdot (\mathbf{r}_{n_2 i_2} - \mathbf{r}_{n_1 i_1}) = \sum_{v} k_{v} [2\pi (l_{v}^{(2)} - l_{v}^{(1)}) + \sum_{\alpha} b_{v}^{\alpha} (\rho_{i_2}^{\alpha} - \rho_{i_1}^{\alpha})].$$
 (18)

So, the overlap matrix $S_{n_i i_i \delta_i, n_j i_j \delta_j}$ is found from the formula

$$S_{n_1i_1\delta_1,n_2i_2\delta_2} = \iiint \psi_{n_1i_1\delta_1}^*(r_1,\theta_1,\phi_1)\psi_{n_2i_2\delta_2}(r_2,\theta_2,\phi_2)r_1^2 \sin\theta_1 dr_1 d\theta_1 d\phi_1, \quad (19)$$

where r_2 , θ_2 , and ϕ_2 are expressed through r_1 , θ_1 , and ϕ_1 in accordance with the following formulae:

$$\mathbf{r}_1 = \mathbf{r} - \mathbf{r}_{n,i}$$
, $\mathbf{r}_2 = \mathbf{r} - \mathbf{r}_{n,i} = \mathbf{r}_1 - \mathbf{r}_{n,i,n,i}$, (20)

$$r_{2} = ((x^{1} - x_{n_{2}i_{2}n_{1}i_{1}}^{1})^{2} + (x^{2} - x_{n_{2}i_{2}n_{1}i_{1}}^{2})^{2} + (x^{3} - x_{n_{2}i_{2}n_{1}i_{1}}^{3})^{2})^{1/2},$$

$$x^{1} = r_{1} \sin \theta_{1} \cos \phi_{1}, \quad x^{2} = r_{1} \sin \theta_{1} \sin \phi_{1}, \quad x^{3} = r_{1} \cos \theta_{1},$$

$$x_{n_{2}i_{2}n_{1}i_{1}}^{\alpha} = \sum_{\nu} (l_{\nu}^{(2)} - l_{\nu}^{(1)}) a_{\nu}^{\alpha} + \rho_{i_{2}}^{\alpha} - \rho_{i_{1}}^{\alpha},$$
(21)

$$\cos \theta_2 = (r_1 \cos \theta_1 - x_{n_2 i_2 n_1 i_1}^3) / r_2, \tag{22}$$

$$\varphi_2 = \arccos((r_1 \sin \theta_1 \cos \varphi_1 - x_{n_2 i_2 n_1 i_1}^1) / (r_2 / (1 - \cos^2 \theta_2)^{1/2})). \tag{23}$$

In formula (21), one should set $x_{n_2i_2n_1i_1}^3=0$ for 2D crystals and $x_{n_2i_2n_1i_1}^2=x_{n_2i_2n_1i_1}^3=0$ for 1D crystals. Summation over n_2 on the right-hand side of formula (16) is reduced

Summation over n_2 on the right-hand side of formula (16) is reduced to a simple summation over integer coordinates $l_{\nu}^{(2)}$, following Eq. (14): $\mathbf{r}_n = (l_1, l_2, l_3)$. Since the matrix element $S_{n_i i_1 \delta_1, n_2 i_2 \delta_2}$ decreases with the distance between the sites $n_1 i_1$, $n_2 i_2$, in numerical calculations, when summing over n_2 in Eq. (16), it is sufficient to restrict ourselves to a few coordination spheres.

Using Eq. (16), the matrix $S_{i_1\delta_1,i_2\delta_2}^{-1/2}(\mathbf{k})$ can be found. So, the matrix $S_{n_2i_2\delta_2,n_1i_1\delta_1}^{-1/2}$ in expression (15) is found from the formula

$$S_{n_1 i_1 \delta_1, n_2 i_2 \delta_2}^{-1/2} = \frac{1}{N} \sum_{\mathbf{k}} S_{i_1 \delta_1, i_2 \delta_2}^{-1/2}(\mathbf{k}) \exp(-i\mathbf{k} \cdot (\mathbf{r}_{n_2 i_2} - \mathbf{r}_{n_1 i_1})). \tag{24}$$

Upon receipt of expressions (3), (6), and (7), it was taken into account that the potential-energy operator for the electron in the field of atomic nuclei can be expressed as

$$\sum_{r^i} v^{ni}(\mathbf{r} - \mathbf{r}'_{ni}), \text{ where } \mathbf{r}'_{ni} = \mathbf{r}_{ni} + \mathbf{u}^{\text{s}}_{ni} + \mathbf{u}_{ni},$$

 \mathbf{r} is the electron-position radius vector, \mathbf{r}_{ni} is the radius vector of atomic nucleus at the equilibrium position in the site (ni) of the crystal lattice, \mathbf{u}_{ni}^{s} is the vector of nucleus static displacement from the equilibrium position in the site (ni), \mathbf{u}_{ni} is the nucleus-displacement operator at the site (ni).

Expanding $v^{ni}(\mathbf{r} - \mathbf{r}'_{ni})$ into a series in powers of $u_{ni\alpha}$ and restricting ourselves to linear terms, we can obtain expressions (3), (6), (7).

The values $h_{n_1i_1\gamma_1,n_2i_2\gamma_2}^{(0)}$ in Eq. (3) are the matrix elements of the kinetic and potential energy $\sum_{n_i} v^{n_i} (\mathbf{r} - \mathbf{r}_{n_i})$ of electron in the field of atomic nuclei in ideal ordered crystal:

$$h_{n_{1}i_{1}\gamma_{1},n_{2}i_{2}\gamma_{2}}^{(0)} = \\ = \sum_{\substack{n_{3}i_{3}\delta_{3}\\n_{1}i_{3}\delta_{3}}} \left(S_{n_{3}i_{3}\delta_{3},n_{1}i_{1}\delta_{1}}^{-1/2}\right)^{*} S_{n_{4}i_{4}\delta_{4},n_{2}i_{2}\delta_{2}}^{-1/2} \left(E_{i_{3}\tilde{\varepsilon}_{3}}S_{n_{3}i_{3}\delta_{3},n_{4}i_{4}\delta_{4}} + \sum_{n_{3}i_{5}\neq n_{3}i_{3}} \upsilon_{n_{3}i_{3}\delta_{3},n_{4}i_{4}\delta_{4}}^{n_{5}i_{5}}\right) \delta_{\sigma_{1}\sigma_{2}}$$
 (25)

 $(\gamma \equiv (\delta \sigma))$. The values here are equal as follow:

$$v_{n_{1}i_{\delta_{1}},n_{2}i_{\delta_{2}}}^{n_{3}i_{3}} = \iiint \psi_{n_{1}i_{\delta_{1}}}^{*}(r_{1},\theta_{1},\phi_{1})v_{n_{3}i_{3}}^{n_{3}i_{3}}\psi_{n_{2}i_{2}\delta_{2}}(r_{2},\theta_{2},\phi_{2})r_{1}^{2}\sin\theta_{1}dr_{1}d\theta_{1}d\phi_{1}, \qquad (26)$$

$$v^{n_3 i_3}(r_3) = -\frac{Z_{i_3} e^2}{r_3}, E_{i_3 \tilde{\varepsilon}_3} = -\frac{m e^4 Z_{i_3}^2}{2 \hbar^2 \tilde{\varepsilon}_3^2}, \tilde{\varepsilon}_3 = 1, 2, 3, \dots$$
 (27)

Here, r_2 , θ_2 , and ϕ_2 are expressed through r_1 , θ_1 , and ϕ_1 following formulae (20)–(23). The expression for r_3 is obtained from expression (21) for r_2 be means of the replacement of $x^{\alpha}_{n_2i_2,n_1i_1}$ with $x^{\alpha}_{n_3i_3,n_1i_1}$; m and e are the mass and charge of the electron, respectively, Z_i are the atomic number of an atom of the λ sort located at the site (ni) of an ideally ordered crystal, and \hbar denotes the Planck's constant.

The matrix element of the electron-nucleus-interaction Hamiltonian in Eq. (6) is given by

$$w_{ni\gamma,n'i'\gamma'} = \sum_{n',n'} w_{ni\gamma,n'i'\gamma'}^{n'i'}, \qquad (28)$$

$$w_{ni\gamma,n'i'\gamma'}^{n^*i''} = \sum_{\lambda} c_{n^*i''}^{\lambda} w_{ni\gamma,n'i'\gamma'}^{\lambda n^*i''}, w_{ni\gamma,n'i'\gamma'}^{\lambda n^*i'} = v_{ni\gamma,n'i'\gamma'}^{\lambda n^*i'} + \Delta v_{ni\gamma,n'i'\gamma'}^{s\lambda n^*i'} - v_{ni\gamma,n'i'\gamma'}^{i'}.$$
 (29)

The symbol $v_{ni\gamma,n'i'\gamma'}^{\lambda n'i'}$ denotes the matrix element of the potential energy $v^{\lambda}(\mathbf{r}-\mathbf{r}_{n'i'})$ of an electron in the field of the nucleus at the site (n''i'') of the crystal:

$$v_{n_{1}i_{1}\gamma_{1},n_{2}i_{2}\gamma_{2}}^{\lambda n_{3}i_{3}} = \iiint \tilde{\psi}_{n_{1}i_{1}\delta_{1}}^{*}(r_{1},\theta_{1},\phi_{1})v_{n_{3}i_{3}}^{\lambda n_{3}i_{3}}(r_{3})\tilde{\psi}_{n_{2}i_{2}\delta_{2}}(r_{2},\theta_{2},\phi_{2})r_{1}^{2}\sin\theta_{1}dr_{1}d\theta_{1}d\phi_{1}\delta_{\sigma_{1}\sigma_{2}},$$

$$v^{\lambda n_{3}i_{3}}(r_{3}) = -\frac{Z_{\lambda}e^{2}}{r_{2}}.$$
(30)

In Eq. (29), c_{ni}^{λ} is a discrete binary random number taking the values of 1 or 0 depending on whether an atom of the λ sort is at the site (ni) or not, respectively.

The term $\Delta v_{ni\gamma,n'i\gamma'}^{s\lambda n''i'}$ in Eq. (29) describes electron scattering on the static displacements of the atoms and is defined by the equation

$$\Delta \nu_{nl\gamma,n'l'\gamma'}^{\mathrm{s}\lambda n''l'} = \sum_{\alpha} \nu_{nl\gamma,n'l'\gamma'}^{\prime\lambda n'l'\alpha} u_{n'l'\alpha}^{\mathrm{s},\lambda}, \qquad (31)$$

where $u_{n'i'\alpha}^{s,\lambda}$ is the α -projection of the static displacement of the atomic nucleus of the λ sort at the site (n''i'') caused by the difference in the nuclei charges of the disordered crystal. In Eq. (31), the value of $v_{ni\gamma,n'i'\gamma}^{\prime\lambda n''i'\alpha}$ is the matrix element of the following operator:

$$-e_{n''i''\alpha}\frac{d}{d\left|\mathbf{r}-\mathbf{r}_{c''i'}\right|}v^{\lambda}\left(\left|\mathbf{r}-\mathbf{r}_{n''i'}\right|\right);\tag{32}$$

$$e_{n''i'} = \frac{\mathbf{r} - \mathbf{r}_{n'i'}}{\left|\mathbf{r} - \mathbf{r}_{n''i'}\right|}.$$
(33)

The expression for $v_{ni\gamma,n'i'\gamma'}^{\lambda n'i'\alpha}$ is obtained from formula (30) by replacing $v^{\lambda n_3i_3}(r_3)$ in it with

$$-\frac{(x^{\alpha}-x_{n_3i_3n_1i_1}^{\alpha})}{r_3}\frac{d}{dr_3}v^{\lambda n_3i_3}(r_3)=-(x^{\alpha}-x_{n_3i_3n_1i_1}^{\alpha})\frac{Z_{\lambda}e^2}{r_3^2}.$$
 (34)

The expression for the operator of the electron-phonon interaction in Eq. (7) is found through derivatives of the potential energy of the electron in the field of atomic nuclei with respect to displacements of the nuclei by the vectors $\{\mathbf{u}_{ni}\}$.

The expression for $v_{ni\gamma,n'i'\gamma'}^{\prime\prime,n'i'\alpha}$ is obtained from formulae (30) and (34), in which Z_{λ} should be replaced with $Z_{i,\cdot}$.

The matrix of the force constants in the expression (9) arising from the direct Coulomb interaction of the atomic nuclei of the disordered crystal has the following form:

$$\Phi_{ni\alpha,n'i'\alpha'} = -\frac{Z_{ni}Z_{n'i'}e^2}{4\pi\epsilon_0 \left|\mathbf{r}_n + \mathbf{\rho}_i - \mathbf{r}_{n'} - \mathbf{\rho}_i'\right|^5} \times$$
(35)

$$\times \left\{3(r_{n\alpha}+\rho_{i\alpha}-r_{n'\alpha}+\rho_{i'\alpha})(r_{n\alpha'}+\rho_{i\alpha'}-r_{n'\alpha'}+\rho_{i'\alpha'})-\left|\mathbf{r}_{n}+\boldsymbol{\rho}_{i}-\mathbf{r}_{n'}-\boldsymbol{\rho}_{i'}\right|^{2}\delta_{\alpha\alpha'}\right\},\ ni\neq n'i',$$

where Z_{ni} is the serial number of the atom located at the lattice site (ni) of the disordered crystal, which is given by the expression

$$Z_{ni} = \sum_{\lambda} c_{ni}^{\lambda} Z_{\lambda}. \tag{36}$$

This matrix $\Phi_{nia,n'i'a'}$ satisfies the following constraint:

$$\sum_{n'i'} \Phi_{ni\alpha,n'i'\alpha'} = 0. \tag{37}$$

Multicentre integrals $v_{n_3,n_4}^{(2)n_1,n_2}$, $n=(ni\gamma)$ in Eq. (8) can be represented as

$$v_{n_{3}i_{3}\gamma_{3},n_{4}i_{4}\gamma_{4}}^{(2)n_{1}i_{1}\gamma_{1},n_{2}i_{2}\gamma_{2}} = e^{2}\delta_{\sigma_{1}\sigma_{4}}\delta_{\sigma_{2}\sigma_{3}}\iint \frac{1}{|\mathbf{r}'-\mathbf{r}''|}\tilde{\Psi}_{n_{1}i_{1}\delta_{1}}^{*}(r_{1}',\theta_{1}',\phi_{1}')\tilde{\Psi}_{n_{2}i_{2}\delta_{2}}^{*}(r_{1}'',\theta_{1}'',\phi_{1}'')\times \times \tilde{\Psi}_{n_{3}i_{3}\delta_{3}}(r_{2}'',\theta_{2}'',\phi_{2}'')\tilde{\Psi}_{n_{4}i_{4}\delta_{4}}(r_{2}',\theta_{2}',\phi_{2}')d^{3}r_{1}'d^{3}r_{1}''.$$
(38)

Here,

$$\left|\mathbf{r}'-\mathbf{r}''\right| = \left(\sum_{\alpha} \left(x'^{\alpha}-x''^{\alpha}-x_{n_2i_2n_1i_1}^{\alpha}\right)^2\right)^{1/2},\tag{39}$$

$$d^3r_1' = r_1' \sin \theta_1' dr_1' d\theta_1' d\phi_1', \qquad (40)$$

$$d^{3}r_{1}'' = r_{1}''\sin\theta_{1}''dr_{1}''d\theta_{1}''d\theta_{1}''. \tag{41}$$

When integrating over r'_1 , θ'_1 , φ'_1 in Eq. (38), r'_2 , θ'_2 , φ'_2 should be expressed through r'_1 , θ'_1 , φ'_1 in accordance with Eqs. (20)–(23), in which it is necessary to replace $x^{\alpha}_{n_2i_2n_1i_1}$ with $x^{\alpha}_{n,i,n,i}$. When integrating over r''_1 , θ''_1 , φ''_1

in Eq. (38), r_2'' , θ_2'' , φ_2'' should be expressed through r_1'' , θ_1'' , φ_1'' in accordance with Eqs. (20)–(23) too, in which it is necessary to replace $x_{n_2i_2n_1i_1}^{\alpha}$ with $x_{n_3i_3n_3i_2}^{\alpha}$.

3. Green's Functions for Electrons and Phonons

We use a Green's function-based formalism to perform the calculations. To calculate the two-time Green's functions, through which the energy spectrum and properties of a disordered crystal are defined, the temperature Green's functions and the known relation between the spectral representations of two-time Green's functions and temperature Green's functions are used. The calculation of the temperature Green's functions for a disordered crystal is based on the diagram technique developed in this work, which is a generalization of the diagram technique for homogeneous systems [37].

Ultimately, we need the real-time retarded $(G_r^{AB}(t,t'))$ and advanced $(G_a^{AB}(t,t'))$ Green's functions, which are defined as follows:

$$G_{\rm r}^{AB}(t,t') = -\frac{i}{\hbar} \theta(t-t') \langle [\tilde{A}(t), \tilde{B}(t')] \rangle, G_{\rm a}^{AB}(t,t') = \frac{i}{\hbar} \theta(t'-t) \langle [\tilde{A}(t), \tilde{B}(t')] \rangle$$
(42)

with the operators expressed in the Heisenberg's representation as

$$\tilde{A}(t) = e^{iHt/\hbar} A e^{-iHt/\hbar}.$$
 (43)

Here and hereinafter, the operator H means the operator $H - \mu_e N_e$, where μ_e is the chemical potential of the electrons' subsystem, N_e is the electron number operator:

 $N_e = \sum_{i} a_{niv}^{\dagger} a_{niv}. \tag{44}$

In addition, the commutator or the anticommutator are defined via

$$[A,B] = AB - \eta BA, \tag{45}$$

where $\eta = 1$ for Bose operators A, B, and $\eta = -1$ for Fermi operators. The symbol $\theta(t)$ in Eq. (42) is the Heaviside's unit-step function. The angle brackets $\langle ... \rangle$ denote the thermal averaging concerning the density matrix ρ :

$$\langle A \rangle = \text{Tr}(\rho A) \text{ and } \rho = \exp((\Omega - H)/\Theta).$$
 (46)

Here, Ω is the thermodynamic potential of the system given by definitions $\exp(-\Omega/\Theta) = \text{Tr}(\exp(-H/\Theta))$ and $\Theta = k_B T$ with Boltzmann's constant k_B and the absolute temperature T.

Our procedure for calculating the real-time Green's functions follows the standard one: we first determine the thermal Green's functions (defined below) and then analytically continue them to real time using the conventional spectral relations.

The thermal Green's functions are defined by

$$G^{AB}(\tau, \tau') = -\langle T_{\tau} \tilde{A}(\tau) \tilde{B}(\tau') \rangle, \tag{47}$$

where the imaginary-time operator $\tilde{A}(\tau)$ is derived from the real-time Heisenberg's representation and the substitution $t = -i\hbar\tau$, i.e.,

$$\tilde{A}(\tau) = e^{H\tau} A e^{-H\tau}.$$
 (48)

In addition, the time-ordering operator satisfies the definition

$$T_{\tau}\tilde{A}(\tau)\tilde{B}(\tau') = \theta(\tau - \tau')\tilde{A}(\tau)\tilde{B}(\tau') + \eta\theta(\tau' - \tau)\tilde{B}(\tau')\tilde{A}(\tau) \tag{49}$$

with $\eta = 1$ or -1 for Bose or Fermi *A* and *B* operators, respectively.

By introducing the operator

$$\sigma(\tau) = e^{H_0 \tau} e^{-H \tau} \text{ with } H = H_0 + H_{\text{int}}, \tag{50}$$

we pass on to the interaction representation. By differentiation of this expression for $\sigma(\tau)$ with respect to τ and integrating starting from 0, with the boundary condition $\sigma(0) = 1$, we obtain

$$\sigma(\tau) = T_{\tau} \exp\left(-\int_{0}^{\tau} H_{\rm int}(\tau') d\tau'\right), \tag{51}$$

where $H_{\mathrm{int}}(au)=e^{H_0 au}H_{\mathrm{int}}e^{-H_0 au}$. Employing this result yields

$$\tilde{A}(\tau) = \sigma^{-1}(\tau)A(\tau)\sigma(\tau) \tag{52}$$

with $A(\tau)$ in the Heisenberg's representation with respect to the noninteracting Hamiltonian. Substituting these results into the definition of the temperature Green's function creates the alternate interaction-representation form for the Green's function given by

$$G^{AB}(\tau, \tau') = -\langle T_{-}A(\tau)B(\tau')\sigma(1/\Theta)\rangle_{\alpha}/\langle \sigma(1/\Theta)\rangle_{\alpha}, \qquad (53)$$

where the whole time dependence is with respect to the noninteracting quasi-particles' Hamiltonian and the trace over all states is for the noninteracting states:

$$\langle O \rangle_0 = \operatorname{Tr}(\rho_0 O), \quad \rho_0 = e^{(\Omega_0 - H_0)/\Theta}.$$
 (54)

This last result forms the starting point for the perturbative computation used here.

Expanding the exponent in expression (51) for $\sigma(\tau)$ in a series of powers $H_{\rm int}(\tau)$, substituting the result in Eq. (53) and using Wick's theorem for calculating the temperature Green's functions of disordered crystals, it is possible to formulate a diagram technique [37]. According to Wick's theorem, the average T-product of several operators is represented by the sum of products of possible average T-products of pairs of operators. The sign before each term corresponds to the pairing of the even permutation of Fermi operators. If the Green's function of the system is expressed as a series of diagrams, then the denominator in Eq. (53) will cancel out with the same factor in the numerator. So, the temperature Green's function is expressed as a series of connected diagrams. Summing up the indicated series, using the standard relation between the spectral representations of the temperature and real-time Green's functions, and performing an

analytical continuation on the real axis, we obtain the following equations for the retarded and advanced Green's functions (hereinafter, the indices 'r' and 'a' is suppressed):

$$G^{aa^{+}}(\varepsilon) = G_{0}^{aa^{+}}(\varepsilon) + G_{0}^{aa^{+}}(\varepsilon)(w + \Sigma_{\text{eph}}(\varepsilon) + \Sigma_{\text{ee}}(\varepsilon))G^{aa^{+}}(\varepsilon),$$

$$G^{uu}(\varepsilon) = G_{0}^{uu}(\varepsilon) + G_{0}^{uu}(\varepsilon)(\Delta\Phi + \Sigma_{\text{phe}}(\varepsilon) + \Sigma_{\text{phph}}(\varepsilon))G^{uu}(\varepsilon) + G_{0}^{up}(\varepsilon)\Delta M^{-1}G^{pu}(\varepsilon),$$

$$G^{PP}(\varepsilon) = G_{0}^{PP}(\varepsilon) + G_{0}^{PP}(\varepsilon)\Delta M^{-1}G^{PP}(\varepsilon) + G_{0}^{Pu}(\varepsilon)(\Delta\Phi + \Sigma_{\text{phe}}(\varepsilon) + \Sigma_{\text{phph}}(\varepsilon))G^{uP}(\varepsilon),$$

$$G^{uP}(\varepsilon) = G_{0}^{uP}(\varepsilon) + G_{0}^{uP}(\varepsilon)\Delta M^{-1}G^{PP}(\varepsilon) + G_{0}^{uu}(\varepsilon)(\Delta\Phi + \Sigma_{\text{phe}}(\varepsilon) + \Sigma_{\text{phph}}(\varepsilon))G^{uP}(\varepsilon),$$

$$G^{Pu}(\varepsilon) = G_{0}^{Pu}(\varepsilon) + G_{0}^{Pu}(\varepsilon)(\Delta\Phi + \Sigma_{\text{phe}}(\varepsilon) + \Sigma_{\text{phph}}(\varepsilon))G^{uU}(\varepsilon) + G_{0}^{PP}(\varepsilon)\Delta M^{-1}G^{Pu}(\varepsilon),$$

$$G^{Pu}(\varepsilon) = G_{0}^{Pu}(\varepsilon) + G_{0}^{Pu}(\varepsilon)(\Delta\Phi + \Sigma_{\text{phe}}(\varepsilon) + \Sigma_{\text{phph}}(\varepsilon))G^{uu}(\varepsilon) + G_{0}^{PP}(\varepsilon)\Delta M^{-1}G^{Pu}(\varepsilon),$$

where $\varepsilon = \hbar\omega$; $G^{aa^+}(\varepsilon)$, $G^{uu}(\varepsilon)$, $G^{pp}(\varepsilon)$, $G^{up}(\varepsilon)$, $G^{pu}(\varepsilon)$ are the real-frequency representation of the single-particle Green's function of the electrons, the coordinate—coordinate, momentum—momentum, coordinate—momentum, and momentum—coordinate Green's functions of the phonons, respectively; $\Sigma_{\rm eph}(\varepsilon)$, $\Sigma_{\rm phe}(\varepsilon)$, $\Sigma_{\rm ee}(\varepsilon)$, $\Sigma_{\rm phph}(\varepsilon)$ are the corresponding self-energies (mass operators) for the electron—phonon, phonon—electron, electron—electron, and phonon—phonon interactions, respectively.

The set of Eqs. (55) can be solved numerically with a predetermined accuracy. When the perturbations are small, given by

$$(\epsilon^2 \Delta M/\hbar^2 + \Delta \Phi + \Sigma_{
m phe}(\epsilon) + \Sigma_{
m phph}(\epsilon))_{ni\alpha,n'i'\alpha'} / \Phi_{ni\alpha,n'i'\alpha'}^{(0)} << 1$$
,

then, the solution of the set of Eqs. (55) becomes

$$G^{aa^{+}}(\varepsilon) = G_{0}^{aa^{+}}(\varepsilon) + G_{0}^{aa^{+}}(\varepsilon)(w + \Sigma_{\text{orb}}(\varepsilon) + \Sigma_{\text{ee}}(\varepsilon))G^{aa^{+}}(\varepsilon), \qquad (56)$$

$$G^{uu}(\varepsilon) = G_0^{uu}(\varepsilon) + G_0^{uu}(\varepsilon)(\Sigma_M(\varepsilon) + \Delta\Phi + \Sigma_{\text{phe}}(\varepsilon) + \Sigma_{\text{phph}}(\varepsilon))G^{uu}(\varepsilon), \quad (57)$$

$$\Sigma_{M n i \alpha, n' i' \alpha'}(\varepsilon) = \frac{\hbar^2}{\varepsilon^2} \sum_{n_1 i_1 \alpha_1} \Phi_{n i \alpha, n_1 i_1 \alpha_1}^{(0)} \left(\frac{1}{M_{n_1 i_1}} - \frac{1}{M_{i_1}} \right) \Phi_{n_1 i_1 \alpha_1, n' i' \alpha'}^{(0)}.$$
 (58)

Using the equations of motion for the Green's functions, one can obtain expressions for the 0th-order Green's functions [26], namely:

$$G_0^{aa^+}(\varepsilon) = (\varepsilon - H_0^{(1)})^{-1},$$
 (59)

where

$$H_0^{(1)} = \left\| h_{ni\gamma, n'i'\gamma'}^{(0)} \right\|,\tag{60}$$

$$G_0^{uu}(\varepsilon) = (\varepsilon^2 M^{(0)}/\hbar^2 - \Phi^{(0)})^{-1},$$
 (61)

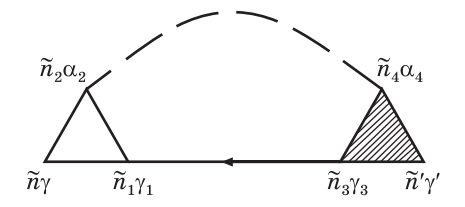
$$\Phi^{(0)} = \left\| \Phi^{(0)}_{ni\alpha, n'i'\alpha'} \right\|,\tag{62}$$

$$\boldsymbol{M}^{(0)} = \left\| \boldsymbol{M}_{i} \boldsymbol{\delta}_{nn'} \boldsymbol{\delta}_{ii'} \boldsymbol{\delta}_{\alpha\alpha'} \right\|. \tag{63}$$

Here, the double vertical bars denote a matrix.

Fig. 1. Diagram for $\Sigma_{\text{eph }ni\gamma,n'i'\gamma'}(\tau,\tau') = \Sigma_{\text{eph }\tilde{n}\gamma,\tilde{n}'\gamma'}$ [30, 31]

The real-time and real-frequency Green's functions are related by standard Fourier-transform relations given by



$$G_{\mathrm{r,a}}^{AB}(t) = \frac{1}{2\pi} \int_{-\infty}^{\infty} G_{\mathrm{r,a}}^{AB}(\omega) e^{-i\omega t} d\omega, \qquad (64)$$

$$G_{\mathrm{r,a}}^{AB}(\omega) = \int_{-\infty}^{\infty} G_{\mathrm{r,a}}^{AB}(t)e^{i\omega t}dt.$$
 (65)

The temperature Green's functions are periodic (for bosons) or antiperiodic (for fermions) on the interval $-1/\Theta \le \tau < 1/\Theta$, and hence, have a Fourier-series representation in terms of their Matsubara's frequencies, as follows:

$$G^{AB}(\tau) = \Theta \sum_{\omega_n} G^{AB}(\omega_n) e^{-i\omega_n \tau}, \tag{66}$$

$$G^{AB}(\omega_n) = \frac{1}{2} \int_{-1/\Theta}^{1/\Theta} G^{AB}(\tau) e^{i\omega_n \tau} d\tau, \qquad (67)$$

where the Matsubara's frequencies meet the conditions

$$\omega_n = \begin{cases} 2n\pi\Theta \text{ for Bose particles,} \\ (2n+1)\pi\Theta \text{ for Fermi particles,} \end{cases} (n = 0, \pm 1, \pm 2, \ldots).$$
 (68)

The electrons' Green's functions are infinite matrices with indices given by the lattice unit cell n, the basis site i within it, and the other quantum numbers γ . Similarly, the phonons' Green's functions are also infinite matrices with the same dependences on lattice unit cells and basis sites, plus a dependence on the spatial coordinate directions α .

The mass operator of the Green's function of electrons for the electron-phonon interactions $\Sigma_{\rm eph}(\tau,\tau')$ is described by the diagram in Fig. 1 (from here, $\tilde{n}=(ni\tau)$). Solid lines in Fig. 1 correspond to the Green's function of electrons $G^{aa^+}_{ni\gamma,n'i\gamma'}(\tau,\tau')$, and dashed lines correspond to the Green's function of phonons $G^{uu}_{ni\alpha,n'i\alpha'}(\tau,\tau')$. The vertex part $\Gamma^{n_2i_2\alpha_2}_{ni\gamma,n_ii\gamma_1}(\tau_2,\tau,\tau_1)$ is described by the diagrams in Fig. 2. The unshaded triangle in Fig. 2 corresponds to the equation

$$\Gamma_{0 \ ni\gamma, n_1 i_1 \gamma_1}^{n_2 i_2 \alpha_2}(\tau_2, \tau, \tau_1) = v_{ni\gamma, n_1 i_1 \gamma_1}^{n_2 i_2 \alpha_2} \delta(\tau - \tau_2) \delta(\tau - \tau_1). \tag{69}$$

In Figures 1 and 2, the summation is performed over the interior points $\tilde{n}\gamma$, $\tilde{n}\alpha$, ..., and implies the summation over $ni\gamma$, $ni\alpha$, ..., and integration over τ . The expressions corresponding to each diagram are multiplied

$$\widetilde{n}_{2}\alpha_{2}$$

$$\widetilde{n}_{2}\alpha_{2}$$

$$\widetilde{n}_{2}\alpha_{2}$$

$$\widetilde{n}_{3}\gamma_{3}$$

$$\widetilde{n}_{4}\gamma_{4}$$

$$\widetilde{n}_{3}\gamma_{5}$$

$$\widetilde{n}_{1}\gamma_{1}$$

$$\widetilde{n}_{2}\alpha_{2}$$

$$\widetilde{n}_{6}\gamma_{6}$$

$$\widetilde{n}_{6}\gamma_{6}$$

$$\widetilde{n}_{1}\gamma_{1}$$

$$\widetilde{n}_{2}\alpha_{2}$$

$$\widetilde{n}_{1}\gamma_{1}$$

$$\widetilde{n}_{2}\gamma_{2}$$

$$\widetilde{n}_{2}\gamma_{2$$

Fig. 3. Diagram for $\Sigma_{\text{phe }ni\alpha,n'i'\alpha'}(\tau,\tau') = \Sigma_{\text{phe }\tilde{n}\alpha,\tilde{n}'\alpha'}$. Here and in the next figures, $\tilde{n} = (ni\tau)$ [30, 31]

Fig. 4. Diagram for
$$\Sigma_{\text{ee }ni\gamma,n'i'\gamma'}(\tau,\tau') = \Sigma_{\text{ee }\tilde{n}\gamma,\tilde{n}'\gamma'}$$
 [30, 31]

by $(-1)^{N+F}$, where N is the order of the diagram (namely, the number of vertices Γ_0 in the diagram), and F is the number of lines for the Green's functions of electrons. These functions exit and enter the same vertices.

Thus, the mass operator of the electrons' Green's function for the electron-phonon interactions $\Sigma_{\rm enh}(\epsilon)$ is described by the formula

$$\Sigma_{\text{eph }ni\gamma,n'i'\gamma'}(\varepsilon) = -\frac{1}{4\pi i} \int_{-\infty}^{\infty} d\varepsilon' \text{cth}\left(\frac{\varepsilon'}{2\Theta}\right) \times$$

$$\times \Gamma_{ni\gamma,n_{3}i_{3}\gamma_{3}}^{(0)} (G_{n_{1}i_{1}\alpha_{1},n_{2}i_{2}\alpha_{2}}^{uu}(\varepsilon') - G_{n_{1}i_{1}\alpha_{1},n_{2}i_{2}\alpha_{2}}^{*uu}(\varepsilon')) G_{n_{3}i_{3}\gamma_{3},n_{4}i_{4}\gamma_{4}}^{aa^{+}}(\varepsilon - \varepsilon') \Gamma_{n_{4}i_{4}\gamma_{4},n'i'\gamma'}^{n_{2}i_{2}\alpha_{2}},$$

$$\Gamma_{ni\gamma,n_{3}i_{3}\gamma_{3}}^{(0)} = \nu'_{ni\gamma,n_{3}i_{3}\gamma_{3}}^{*n_{1}i_{1}\alpha_{1}},$$

$$(71)$$

where repeated indices are summed over.

The self-energy of the phonon due to the phonon-electron interactions is given by the expression

$$\Sigma_{\text{phe }ni\alpha,n'i'\alpha'}(\varepsilon) = \frac{1}{2\pi i} \int_{-\infty}^{\infty} d\varepsilon' f(\varepsilon') \times \\ \times \Gamma_{n_{2}i_{2}\gamma_{2},n_{1}i_{1}\gamma_{1}}^{(0) ni\alpha} (G_{n_{1}i_{1}\gamma_{1},n_{3}i_{3}\gamma_{3}}^{aa^{+}}(\varepsilon + \varepsilon') - G_{n_{1}i_{1}\gamma_{1},n_{3}i_{3}\gamma_{3}}^{* aa^{+}}(\varepsilon + \varepsilon')) G_{n_{4}i_{4}\gamma_{4},n_{2}i_{2}\gamma_{2}}^{* aa^{+}}(\varepsilon') + \\ + G_{n_{1}i_{1}\gamma_{1},n_{3}i_{3}\gamma_{3}}^{aa^{+}}(\varepsilon + \varepsilon') (G_{n_{4}i_{4}\gamma_{4},n_{2}i_{2}\gamma_{2}}^{aa^{+}}(\varepsilon') - G_{n_{4}i_{4}\gamma_{4},n_{2}i_{2}\gamma_{2}}^{* aa^{+}}(\varepsilon')) \Gamma_{n_{3}i_{3}\gamma_{3},n_{4}i_{4}\gamma_{4}}^{n'i'\gamma'}$$

insofar as phonon-electron interactions are described by the diagram in Fig. 3. (The designation in Fig. 3 corresponds to designations in Figs. 1, 2.)

From Wick's theorem, it follows that, for a system of electrons with pairwise interactions (Eq. (8)), the mass operator of electron–electron interactions is described by the sum of diagrams. Diagrams for the mass operator $\Sigma_{\rm ee}(\tau,\tau')$ describing the electron–electron interactions are shown in Fig. 4.

Fig. 5. Diagrams for the vertex part
$$\Gamma_{\tilde{n}_{1}\tilde{\gamma}_{1}\tilde{\gamma}_{1}}^{\tilde{n}_{2}\tilde{\gamma}_{2},\tilde{n}_{1}\tilde{\gamma}_{1}}$$
 $\Gamma_{\tilde{n}_{2}\tilde{\gamma}_{2},\tilde{n}_{1}\tilde{\gamma}_{1}}^{\tilde{n}_{1}\tilde{\gamma}_{1}}$ $\Gamma_{\tilde{n}_{2}\tilde{\gamma}_{2},\tilde{n}_{1}\tilde{\gamma}_{1}}^{\tilde{n}_{1}\tilde{\gamma}_{1}}$ $\Gamma_{\tilde{n}_{2}\tilde{\gamma}_{2},\tilde{n}_{1}\tilde{\gamma}_{1}}^{\tilde{n}_{1}\tilde{\gamma}_{1}}$ $\Gamma_{\tilde{n}_{1}\tilde{\gamma}_{1}\tilde{\gamma}_{1}}^{\tilde{n}_{2}\tilde{\gamma}_{2},\tilde{n}_{1}\tilde{\gamma}_{1}}$ $\Gamma_{\tilde{n}_{1}\tilde{\gamma}_{1}\tilde{\gamma}_{1}}^{\tilde{n}_{2}\tilde{\gamma}_{2},\tilde{n}_{1}\tilde{\gamma}_{1}}$ $\Gamma_{\tilde{n}_{1}\tilde{\gamma}_{1}\tilde{\gamma}_{1}}^{\tilde{n}_{2}\tilde{\gamma}_{2},\tilde{n}_{1}\tilde{\gamma}_{1}}^{\tilde{n}_{2}\tilde{\gamma}_{2},\tilde{n}_{1}\tilde{\gamma}_{1}}^{\tilde{n}_{2}\tilde{\gamma}_{2},\tilde{n}_{1}\tilde{\gamma}_{1}}^{\tilde{n}_{2}\tilde{\gamma}_{2},\tilde{n}_{1}\tilde{\gamma}_{1}}^{\tilde{n}_{2}\tilde{\gamma}_{2},\tilde{n}_{1}\tilde{\gamma}_{1}}^{\tilde{n}_{2}\tilde{\gamma}_{2},\tilde{n}_{1}\tilde{\gamma}_{1}}^{\tilde{n}_{2}\tilde{\gamma}_{2},\tilde{n}_{1}\tilde{\gamma}_{1}}^{\tilde{n}_{2}\tilde{\gamma}_{2},\tilde{n}_{1}\tilde{\gamma}_{1}}^{\tilde{n}_{2}\tilde{\gamma}_{2},\tilde{n}_{1}\tilde{\gamma}_{1}}^{\tilde{n}_{2}\tilde{\gamma}_{2},\tilde{n}_{1}\tilde{\gamma}_{1}}^{\tilde{n}_{2}\tilde{\gamma}_{2},\tilde{n}_{1}\tilde{\gamma}_{1}}^{\tilde{n}_{2}\tilde{\gamma}_{2},\tilde{n}_{1}\tilde{\gamma}_{1}}^{\tilde{n}_{2}\tilde{\gamma}_{2},\tilde{n}_{1}\tilde{\gamma}_{1}}^{\tilde{n}_{2}\tilde{\gamma}_{2},\tilde{n}_{1}\tilde{\gamma}_{1}}^{\tilde{n}_{2}\tilde{\gamma}_{2},\tilde{n}_{1}\tilde{\gamma}_{1}}^{\tilde{n}_{2}\tilde{\gamma}_{2},\tilde{n}_{1}\tilde{\gamma}_{1}}^{\tilde{n}_{2}\tilde{\gamma}_{2},\tilde{n}_{1}\tilde{\gamma}_{1}}^{\tilde{n}_{2}\tilde{\gamma}_{2},\tilde{n}_{1}\tilde{\gamma}_{1}}^{\tilde{n}_{2}\tilde{\gamma}_{2},\tilde{n}_{1}\tilde{\gamma}_{1}}^{\tilde{n}_{2}\tilde{\gamma}_{2},\tilde{n}_{1}\tilde{\gamma}_{1}}^{\tilde{n}_{2}\tilde{\gamma}_{2},\tilde{n}_{1}\tilde{\gamma}_{1}}^{\tilde{n}_{2}\tilde{\gamma}_{2},\tilde{n}_{1}\tilde{\gamma}_{1}}^{\tilde{n}_{2}\tilde{\gamma}_{2},\tilde{n}_{1}\tilde{\gamma}_{1}}^{\tilde{n}_{2}\tilde{\gamma}_{2},\tilde{n}_{1}\tilde{\gamma}_{1}}^{\tilde{n}_{2}\tilde{\gamma}_{2},\tilde{n}_{1}\tilde{\gamma}_{1}}^{\tilde{n}_{2}\tilde{\gamma}_{2},\tilde{n}_{1}\tilde{\gamma}_{1}}^{\tilde{n}_{2}\tilde{\gamma}_{2},\tilde{n}_{1}\tilde{\gamma}_{1}}^{\tilde{n}_{2}\tilde{\gamma}_{2},\tilde{n}_{1}\tilde{\gamma}_{1}}^{\tilde{n}_{2}\tilde{\gamma}_{2},\tilde{n}_{1}\tilde{\gamma}_{1}}^{\tilde{n}_{2}\tilde{\gamma}_{2},\tilde{n}_{1}\tilde{\gamma}_{1}}^{\tilde{n}_{2}\tilde{\gamma}_{2},\tilde{n}_{1}\tilde{\gamma}_{1}}^{\tilde{n}_{2}\tilde{\gamma}_{2},\tilde{n}_{1}\tilde{\gamma}_{1}}^{\tilde{n}_{2}\tilde{\gamma}_{2},\tilde{n}_{1}\tilde{\gamma}_{1}}^{\tilde{n}_{2}\tilde{\gamma}_{2},\tilde{n}_{1}\tilde{\gamma}_{1}}^{\tilde{n}_{2}\tilde{\gamma}_{2},\tilde{n}_{1}\tilde{\gamma}_{1}}^{\tilde{n}_{2}\tilde{\gamma}_{2},\tilde{n}_{1}\tilde{\gamma}_{1}}^{\tilde{n}_{2}\tilde{\gamma}_{2},\tilde{n}_{1}\tilde{\gamma}_{1}}^{\tilde{n}_{2}\tilde{\gamma}_{2},\tilde{n}_{1}\tilde{\gamma}_{1}}^{\tilde{n}_{2}\tilde{\gamma}_{2},\tilde{n}_{1}\tilde{\gamma}_{1}}^{\tilde{n}_{2}\tilde{\gamma}_{2},\tilde{n}_{1}\tilde{\gamma}_{1}}^{\tilde{n}_{2}\tilde{\gamma}_{2},\tilde{n}_{1}\tilde{\gamma}_{1}}^{\tilde{n}_{2}\tilde{\gamma}_{2},\tilde{n}_{1}\tilde{\gamma}_{1}}^{\tilde{n}_{2}\tilde{\gamma}_{2},\tilde{n}_{1}\tilde{\gamma}_{1}}^{\tilde{n}_{2}\tilde{\gamma}_{2},\tilde{n}_{1}\tilde{\gamma}_{1}}^{\tilde{n}_{2}\tilde{\gamma}_{2$

The vertex parts $\Gamma_{ni\gamma,n'i\gamma'}^{n_2i\gamma_2,n_1i_1\gamma_1}(\tau_2,\tau_1,\tau,\tau')$ are shown on diagrams in Fig. 5. The unshaded triangle in Fig. 5 corresponds to the equation

$$\Gamma_{niv,n'i'v'}^{(0) n_2 i_2 \gamma_2, n_i i_1 \gamma_1}(\tau_2, \tau_1, \tau, \tau') = \Gamma_{n,n'}^{(0) n_2, n_1} \delta(\tau - \tau_2) \delta(\tau - \tau_1) \delta(\tau - \tau'), \tag{73}$$

$$\Gamma_{n,n'}^{(0) n_2,n_1} = (v_{n_1,n'}^{(2) n,n_2} - v_{n',n_1}^{(2) n,n_2})/2.$$
(74)

The mass operator describing electron-electron interactions is

$$\Sigma_{\text{ee }n,n'}(\varepsilon) = \Sigma_{\text{ee }n,n'}^{(1)}(\varepsilon) + \Sigma_{\text{ee }n,n'}^{(2)}(\varepsilon), \tag{75}$$

$$\Sigma_{\text{ee }n,n'}^{(1)}(\varepsilon) = -\frac{1}{2\pi i} \int_{-\infty}^{\infty} d\varepsilon' f(\varepsilon') \Gamma_{n,n'}^{n_2,n_1}(G_{n_1,n_2}^{aa^+}(\varepsilon') - G_{n_1,n_2}^{*aa^+}(\varepsilon')), \qquad (76)$$

$$\Sigma_{\text{ee}\,n,n'}^{(2)}(\varepsilon) = -\frac{1}{2} \left(\frac{1}{2\pi i}\right)^{2} \int_{-\infty}^{\infty} d\varepsilon_{1} \int_{-\infty}^{\infty} d\varepsilon_{2} f(\varepsilon_{1}) f(\varepsilon_{2}) \times \\ \times \Gamma_{n_{2},n_{1}}^{(0)\,n,n_{3}} \left[(G_{n_{2},n_{5}}^{aa^{+}}(\varepsilon - \varepsilon_{1} - \varepsilon_{2}) G_{n_{1},n_{4}}^{*\,aa^{+}}(\varepsilon_{1}) - G_{n_{2},n_{5}}^{*\,aa^{+}}(\varepsilon - \varepsilon_{1} - \varepsilon_{2}) G_{n_{1},n_{4}}^{aa^{+}}(\varepsilon_{1}) \right) \times \\ \times (G_{n_{6},n_{3}}^{aa^{+}}(\varepsilon_{2}) - G_{n_{6},n_{3}}^{*\,aa^{+}}(\varepsilon_{2})) - (G_{n_{2},n_{5}}^{aa^{+}}(\varepsilon - \varepsilon_{1} - \varepsilon_{2}) - G_{n_{2},n_{5}}^{*\,aa^{+}}(\varepsilon - \varepsilon_{1} - \varepsilon_{2})) \times \\ \times (G_{n_{1},n_{4}}^{aa^{+}}(\varepsilon_{1}) G_{n_{6},n_{3}}^{aa^{+}}(\varepsilon_{2}) - G_{n_{1},n_{4}}^{*\,aa^{+}}(\varepsilon_{1}) G_{n_{6},n_{3}}^{*\,aa^{+}}(\varepsilon_{2})) \right] \Gamma_{n_{4},n^{6}}^{n_{5},n_{6}}.$$

Formula (75) for the mass operator of the electron-electron interactions follows from the symmetrisation of the exponent in the right-hand side of Eq. (51) by the indices of the quantum states of the Hamiltonian of the electron-electron interactions (8).

The second diagram in Fig. 4 is multiplied by 1/2 (see expression (77) for the mass operator of the electron–electron interactions).

A similar result for the contribution to the phonon self-energy $\Sigma_{phph}(\epsilon)$ from phonon–phonon couplings is given in Ref. [33]. Summation is implied over repeated indices in these expressions.

In Eqs. (69)–(77), $\Gamma_{n_3i_3\gamma_3,n_4i_4\gamma_4}^{n'i'a'}$, $\Gamma_{n_4,n'}^{n_5,n_6}$ are the vertex parts of the mass operators of electron–phonon, phonon–electron, and electron–electron interactions. They are represented as infinite series in powers of the matrix elements of the operators describing these interactions. The renormalization of the vertex parts in the expressions (69)–(77) for mass operators can be performed using the diagrams proposed in Ref. [30]. We will get the following equations:

$$\Gamma_{n_3i_3\gamma_3,n_4i_4\gamma_4}^{n'i'\gamma'}=\Gamma_{n_3i_3\gamma_3,n_4i_4\gamma_4}^{(0)\;n'i'lpha'}-rac{1}{2\pi i}\int\limits_{-\infty}^{\infty}d\epsilon f(\epsilon) imes$$

$$\times\Gamma_{n_{5}i_{5}\gamma_{5},n_{6}i_{6}\gamma_{6}}^{(0)n'i'\alpha'}(G_{n_{6}i_{6}\gamma_{6},n_{7}i_{7}\gamma_{7}}^{aa^{+}}(\varepsilon)G_{n_{8}i_{8}\gamma_{8},n_{5}i_{5}\gamma_{5}}^{aa^{+}}(\varepsilon) - G_{n_{6}i_{6}\gamma_{6},n_{7}i_{7}\gamma_{7}}^{*aa^{+}}(\varepsilon)G_{n_{8}i_{8}\gamma_{8},n_{5}i_{5}\gamma_{5}}^{*aa^{+}}(\varepsilon)) \times \\ \times\Gamma_{n_{7}i_{7}\gamma_{7},n_{8}i_{8}\gamma_{8}}^{(0)n_{9}i_{9}\alpha_{9}}G_{n_{9}i_{9}\gamma_{9},n_{10}i_{10}\gamma_{10}}^{uu}(0)\Gamma_{n_{3}i_{3}\gamma_{3},n_{4}i_{4}\gamma_{4}}^{*n_{10}i_{10}\alpha_{10}},$$

$$(78)$$

$$\Gamma_{n_4,n'}^{n_5,n_6} = \Gamma_{n_4,n'}^{(0) n_5,n_6} -$$

$$-\frac{1}{2\pi i} \int_{-\infty}^{\infty} d\varepsilon f(\varepsilon) \Gamma_{n_4,n_8}^{(0) n_5,n_7} (G_{n_7,n_9}^{aa^+}(\varepsilon) G_{n_8,n_{10}}^{* aa^+}(\varepsilon) - G_{n_7,n_9}^{* aa^+}(\varepsilon) G_{n_8,n_{10}}^{aa^+}(\varepsilon)) \Gamma_{n_1,n_7}^{n_9,n_6}. \quad (79)$$

In deriving the expressions in Eqs. (70), (72), (76), and (77), we employed the standard techniques for an arbitrary function $\phi(z)$, which is analytic in the region covered by the contour C enclosing all the Matsubara's frequencies. Namely, we have

$$\Theta \sum_{\omega_n} \phi(i\omega_n) = \frac{1}{4\pi i} \oint_C dz \, \text{cth} \left(z/(2\Theta) \right) \phi(z) \, \left(\omega_n = 2n\pi\Theta \right) \tag{80}$$

for the bosonic case, and

$$\Theta \sum_{\omega_{n}} \phi(i\omega_{n}) = -\frac{1}{2\pi i} \oint_{C} dz \tilde{f}(z/\Theta) \phi(z) (\omega_{n} = (2n+1)\pi\Theta)$$
 (81)

for the fermionic case, where

$$\tilde{f}\left(z/\Theta\right) = \left(\exp(z/\Theta) + 1\right)^{-1}.\tag{82}$$

It should be noted that the first term in the electron self-energy due to electron–electron interactions, $\Sigma^{(1)}_{\text{ee}\,n,n'}(\epsilon)$ in Eq. (75), describes the Coulomb and exchange electron–electron interactions within the Hartree–Fock approximation. The second term, $\Sigma^{(2)}_{\text{ee}\,n,n'}(\epsilon)$, which is caused by corrections beyond Hartree–Fock approximation, describes the effects of electron correlations. As opposed to the procedures used in Refs. [12, 13], the long-range Coulomb interaction of electrons located at different crystal-lattice sites is described by taking into account an arbitrary number of energy bands.

4. Number of Electrons and Magnetic Moments of Atoms

The Fermi level µ of the system is determined by the equations

$$\langle Z \rangle = \int_{-\infty}^{\infty} f(\varepsilon) g_{\rm e}(\varepsilon) d\varepsilon, \tag{83}$$

$$f(\varepsilon) = (\exp(\varepsilon - \mu)/\Theta + 1)^{-1}, \tag{84}$$

where $\langle Z \rangle$ is the average number of electrons per atom and $g_{\rm e}(\epsilon)$ is the electron density of states, which satisfies the condition

$$g_{e}(\varepsilon) = -\frac{1}{\pi v N} \operatorname{Im} \operatorname{Tr} \langle G^{aa^{+}}(\varepsilon) \rangle. \tag{85}$$

Here, $\langle ... \rangle$ denotes configurational averaging over the disorder, N is the

number of primitive unit cells in the lattice, and v is the number of sites per primitive unit cell.

The obtained expressions for the Green's functions (56), (57) are also valid if, in addition to concentration fluctuations, the crystal contains the charge and spin density fluctuations. Since we will be using with number of electrons per atom and magnetic moment further, we now slightly modify our notation so that the symbol $\gamma \equiv (\delta \sigma) = (\tilde{\epsilon} lm\sigma)$ refers to all other quantum numbers except for spin, and we will introduce the spin quantum number σ explicitly in all following equations.

The electron-electron self-energy in Eq. (56) requires the occupation number $Z_{\delta\sigma}^{\lambda ni}$ of the different electron states $(ni\delta\sigma)$, where here we are explicitly including the dependence on σ . The explicit values for $Z_{\delta\sigma}^{\lambda ni}$ are calculated from Eq. (83), where the total electron density of states $g_{\epsilon}(\varepsilon)$ is replaced by the partial density of states $g_{\delta\sigma}^{\lambda ni}(\varepsilon)$ for the energy band δ and spin projection σ to allow for the magnetic solutions. Then, the occupation numbers $Z_{\delta\sigma}^{\lambda ni}$ and the partial density of states $g_{\delta\sigma}^{\lambda ni}(\varepsilon)$ satisfy the following conditions:

$$Z_{\delta\sigma}^{\lambda ni} = \int_{0}^{\infty} f(\varepsilon) g_{\delta\sigma}^{\lambda ni}(\varepsilon) d\varepsilon, \tag{86}$$

$$g_{\delta\sigma}^{\lambda ni}(\varepsilon) = -\frac{1}{\pi} \operatorname{Im} \langle G_{ni\delta\sigma,ni\delta\sigma}^{aa^{+}}(\varepsilon) \rangle \Big|_{(ni)\in\lambda}.$$
 (87)

Note that the disorder averaging is done under the assumption that an atom of the λ sort is located at the site (ni), the number of electrons per atom is equal to Z_{λ} , and the projection of the localized magnetic moment onto the Oz axis is equal to m_{λ} .

The localized magnetic moments inhomogeneously distributed over the crystal lattice sites and the static magnetization fluctuations are described similarly.

The total number of electrons per atom and magnetic moment are given by the following formulae:

$$Z_{\lambda} = \sum_{\delta} Z_{\lambda\delta} , \qquad (88)$$

$$m_{\lambda} = \sum_{\delta} m_{\lambda\delta} , \qquad (89)$$

$$Z_{\lambda\delta} = Z_{\delta\sigma}^{\lambda ni} + Z_{\delta,-\sigma}^{\lambda ni},$$
 (90)

$$m_{\lambda\delta} = m_{\delta\sigma}^{\lambda ni} - m_{\delta,-\sigma}^{\lambda ni} \,. \tag{91}$$

Let us consider the probability of this configuration is P_{ni}^{λ} , and we have the obvious constraint

$$\sum_{\lambda} P_{ni}^{\lambda} = 1. \tag{92}$$

5. Density of Electron and Phonon States in a System

In expressions (56) and (57), we represent each mass operator as a sum of single-site operators and perform a cluster expansion for the Green's functions $G^{aa^{\dagger}}(\varepsilon)$, $G^{uu}(\varepsilon)$, by introducing the Green's functions of the effective medium as a zeroth approximation. The indicated expansions are a generalization of the cluster expansion for the Green's function $G^{aa^{\dagger}}(\varepsilon)$ of the single-particle Hamiltonian [26].

Green's functions of the effective medium are defined by the following expressions:

$$\tilde{G}^{aa^{+}}(\varepsilon) = \left[\varepsilon - H_0^{(1)} - \tilde{\Sigma}_{eph}(\varepsilon) - \tilde{\Sigma}_{ee}(\varepsilon) - \sigma_{e}(\varepsilon)\right]^{-1}, \tag{93}$$

$$\tilde{G}^{uu}(\varepsilon) = \left[\varepsilon^2 M^{(0)}/\hbar^2 - \Phi^{(0)} - \tilde{\Sigma}_{\text{phe}}(\varepsilon) - \tilde{\Sigma}_{\text{phph}}(\varepsilon) - \sigma_{\text{ph}}(\varepsilon)\right]^{-1}.$$
 (94)

Expressions for the operators $\tilde{\Sigma}_{\rm eph}(\epsilon)$, $\tilde{\Sigma}_{\rm phe}(\epsilon)$, $\tilde{\Sigma}_{\rm ee}(\epsilon)$ are obtained from Eqs. (69)–(77) for the mass operators $\Sigma_{\rm eph}(\epsilon)$, $\Sigma_{\rm phe}(\epsilon)$, $\Sigma_{\rm ee}(\epsilon)$ by replacing the Green's functions $G^{aa^+}(\epsilon)$, $G^{uu}(\epsilon)$ with the Green's functions of the effective medium $\tilde{G}^{aa^+}(\epsilon)$, $\tilde{G}^{uu}(\epsilon)$, which satisfy the Dyson equation expressed in terms of the scattering T-matrix [30]:

$$G(\varepsilon) = \tilde{G}(\varepsilon) + \tilde{G}(\varepsilon)T(\varepsilon)\tilde{G}(\varepsilon), \tag{95}$$

where the scattering *T*-matrix is represented by a series, in which each term describes the scattering of clusters with different numbers of sites, expressed schematically as

$$T = \sum_{n_1 i_1} t^{n_1 i_1} + \sum_{n_2 i_2 \neq n_2 i_2} T^{(2) n_1 i_1, n_2 i_2} + \dots$$
 (96)

Here, we have the one-site scattering operator

$$t^{n_1 i_1} = (I - (\sum_{e}^{n_1 i_1} - \sigma^{i_1}) \tilde{G})^{-1} (\sum_{e}^{n_1 i_1} - \sigma^{i_1}).$$
 (97)

and the two-site scattering operator

$$T^{(2) n_1 i_1, n_2 i_2} = (I - t^{n_1 i_1} \tilde{G} t^{n_2 i_2} \tilde{G})^{-1} t^{n_1 i_1} \tilde{G} t^{n_2 i_2} (I + \tilde{G} t^{n_1 i_1}).$$
 (98)

The self-energy employed in Eq. (97), $\sum_{e}^{n_1 i_1}$, satisfies the condition

$$w + \Sigma_{\text{eph}}(\varepsilon) + \Sigma_{\text{ee}}(\varepsilon) - \tilde{\Sigma}_{\text{eph}}(\varepsilon) - \tilde{\Sigma}_{\text{ee}}(\varepsilon) = \sum_{n_1 i_1} \Sigma_{\text{e}}^{n_1 i_1}$$
(99)

for the electrons. For the phonons, we have

$$\Sigma_{M}(\varepsilon) + \Delta\Phi + \Sigma_{\text{phe}}(\varepsilon) + \Sigma_{\text{phph}}(\varepsilon) - \tilde{\Sigma}_{\text{phe}}(\varepsilon) - \tilde{\Sigma}_{\text{phph}}(\varepsilon) = \sum_{n_{1}i_{1}} \Sigma_{\text{ph}}^{n_{1}i_{1}}.$$
 (100)

The expressions for the matrices (coherent potentials) $\sigma_e(\epsilon)$, $\sigma_{ph}(\epsilon)$ in formulae (93) and (94) for the Green's functions of the effective medium will be determined from the condition that there are no contributions from multiple-scattering processes at one site to the configuration-averaged

Green's functions:

$$\langle t^{n_1 i_1} \rangle = 0. \tag{101}$$

The matrix elements of the Green's function of the electrons' subsystem of the effective medium can be calculated using the Fourier transform:

$$\tilde{G}_{ni\gamma,n'i'\gamma'}^{aa^{+}}(\varepsilon) = \frac{1}{N} \sum_{\mathbf{k}} \tilde{G}_{i\gamma,i'\gamma'}^{aa^{+}}(\mathbf{k},\varepsilon) e^{i\mathbf{k}\cdot(\mathbf{r}_{ni}-\mathbf{r}_{n'i'})},$$
(102)

$$\tilde{G}^{aa^{+}}(\mathbf{k},\varepsilon) = (\varepsilon - \tilde{H}(\mathbf{k},\varepsilon))^{-1}, \tag{103}$$

where

$$H(\mathbf{k}, \varepsilon) = \left\| h_{i\gamma, i'\gamma'}^{(0)}(\mathbf{k}) + \tilde{\Sigma}_{\text{eph } i\gamma, i'\gamma'}(\mathbf{k}, \varepsilon) + \tilde{\Sigma}_{\text{ee } i\gamma, i'\gamma'}(\mathbf{k}, \varepsilon) + \sigma_{\text{ei } i\gamma, i'\gamma'}(\mathbf{k}, \varepsilon) \right\|, \quad (104)$$

$$\sigma_{\operatorname{ei} i\gamma, i'\gamma'}(\mathbf{k}, \varepsilon) = \sum_{n'n, i_1} \sigma_{\operatorname{e} n_1 i_1 \gamma, n'i'\gamma'}^{ni}(\varepsilon) e^{-i\mathbf{k}\cdot(\mathbf{r}_{ni} - \mathbf{r}_{n'i'})};$$
(105)

 $\sigma^{ni}_{e \, n_i l_i \gamma, \, n' l' \gamma'}(\epsilon)$ means the matrix element of the coherent potential. We do a similar procedure for the effective-medium phonon Green's function, which satisfies the definitions

$$\tilde{G}^{uu}_{ni\alpha,n'i'\alpha'}(\varepsilon) = \frac{1}{N} \sum_{\mathbf{k}} \tilde{G}^{uu}_{i\alpha,i'\alpha'}(\mathbf{k},\varepsilon) e^{i\mathbf{k}\cdot(\mathbf{r}_{ni}-\mathbf{r}_{n'i'})},$$
(106)

$$\tilde{G}^{uu}(\mathbf{k}, \varepsilon) = (\varepsilon^2 M^{(0)}/\hbar^2 - \tilde{\Phi}(\mathbf{k}, \varepsilon))^{-1}; \qquad (107)$$

$$\tilde{\Phi}(\mathbf{k}, \epsilon) = \left\| \Phi_{i\alpha, i'\alpha'}^{(0)}(\mathbf{k}) + \tilde{\Sigma}_{\text{phe } i\alpha, i'\alpha'}(\mathbf{k}, \epsilon) + \tilde{\Sigma}_{\text{phph } i\alpha, i'\alpha'}(\mathbf{k}, \epsilon) + \sigma_{\text{ph } i\alpha, i'\alpha'}(\mathbf{k}, \epsilon) \right\|, \quad (108)$$

$$\sigma_{\text{ph } i\alpha,i'\alpha'}(\mathbf{k},\varepsilon) = \sum_{n'n_1i_1} \sigma_{\text{ph } n_1i\alpha,n'i'\alpha'}^{ni}(\varepsilon) \exp(i\mathbf{k} \cdot (\mathbf{r}_{n'i'} - \mathbf{r}_{ni})), \tag{109}$$

$$M_{ia,i'a'}^{(0)} = M_i \delta_{ii'} \delta_{aa'}. \tag{110}$$

The Fourier transform of the mass operator of electron-phonon interactions has the form:

$$\tilde{\Sigma}_{\text{eph }i\gamma,i'\gamma'}(\mathbf{k},\varepsilon) = -\frac{1}{4\pi i} \frac{1}{N} \int_{-\infty}^{\infty} d\varepsilon' \text{cth}\left(\varepsilon'/(2\Theta)\right) \sum_{\mathbf{k}_{1}} \Gamma_{i\gamma,i_{3}\gamma_{3}}^{(0) i_{1}\alpha_{1}}(-\mathbf{k},\mathbf{k}-\mathbf{k}_{1}) \times \\
\times (\tilde{G}_{i\alpha_{1},i_{3}\alpha_{3}}^{uu}(\mathbf{k},\varepsilon') - \tilde{G}_{i,\alpha_{1},i_{3}\alpha_{2}}^{*uu}(\mathbf{k},\varepsilon')) \tilde{G}_{i,\alpha_{2},i_{3}\gamma_{3}}^{aa^{+}}(\mathbf{k}-\mathbf{k}_{1},\varepsilon-\varepsilon') \Gamma_{i,\alpha_{2},i_{3}\gamma_{3}}^{i_{2}\alpha_{2}}(-\mathbf{k}+\mathbf{k}_{1},\mathbf{k}).$$
(111)

The Fourier transform of the phonon-electron-interactions' mass operator is as follows:

$$\begin{split} \tilde{\Sigma}_{\text{phe }ni\alpha,n'i'\alpha'}(\mathbf{k},\varepsilon) &= \frac{1}{2\pi i} \frac{1}{N} \int\limits_{-\infty}^{\infty} d\varepsilon_{1} f(\varepsilon_{1}) \sum_{\mathbf{k}_{1}} \Gamma^{(0)}_{i_{2}\gamma_{2},i_{1}\gamma_{1}}(-\mathbf{k}_{1},\mathbf{k}+\mathbf{k}_{1}) \times \\ &\times \{ [\tilde{G}^{aa^{+}}_{i_{1}\gamma_{1},i_{3}\gamma_{3}}(\mathbf{k}+\mathbf{k}_{1},\varepsilon+\varepsilon_{1}) - \tilde{G}^{*}_{i_{1}\gamma_{1},i_{3}\gamma_{3}}(\mathbf{k}+\mathbf{k}_{1},\varepsilon+\varepsilon_{1})] \tilde{G}^{*}_{i_{4}\gamma_{4},i_{2}\gamma_{2}}(\mathbf{k}_{1},\varepsilon_{1}) + \\ &+ \tilde{G}^{aa^{+}}_{i_{1}\gamma_{1},i_{3}\gamma_{3}}(\mathbf{k}+\mathbf{k}_{1},\varepsilon+\varepsilon_{1}) [\tilde{G}^{aa^{+}}_{i_{4}\gamma_{4},i_{2}\gamma_{2}}(\mathbf{k}_{1},\varepsilon_{1}) - \tilde{G}^{*}_{i_{4}\gamma_{4},i_{2}\gamma_{2}}(\mathbf{k}_{1},\varepsilon_{1})] \} \tilde{\Gamma}^{i'\alpha'}_{i_{3}\gamma_{3},i_{4}\gamma_{4}}(-\mathbf{k}-\mathbf{k}_{1},\mathbf{k}_{1}). \end{split}$$

The vertex parts of the mass operators of the electron-phonon and phonon-electron interactions are determined by the equation

$$\Gamma_{i_{1}\gamma_{1},i_{2}\gamma_{2}}^{i'\alpha'}(\mathbf{k}_{1},\mathbf{k}_{2}) = \Gamma_{i_{1}\gamma_{1},i_{2}\gamma_{2}}^{(0)i'\alpha'}(\mathbf{k}_{1},\mathbf{k}_{2}) - \frac{1}{2\pi i} \frac{1}{N} \int_{-\infty}^{\infty} d\varepsilon f(\varepsilon) \times \\ \times \sum_{\mathbf{k}_{3}} \Gamma_{i_{3}\gamma_{3},i_{4}\gamma_{4}}^{(0)i'\alpha'}(\mathbf{k}_{1} + \mathbf{k}_{2} - \mathbf{k}_{3},\mathbf{k}_{3}) [\tilde{G}_{i_{4}\gamma_{4},i_{5}\gamma_{5}}^{aa^{*}}(\mathbf{k}_{3},\varepsilon) \tilde{G}_{i_{6}\gamma_{6},i_{3}\gamma_{3}}^{aa^{*}}(-\mathbf{k}_{1} - \mathbf{k}_{2} + \mathbf{k}_{3},\varepsilon) - \\ -\tilde{G}_{i_{4}\gamma_{4},i_{5}\gamma_{5}}^{*}(\mathbf{k}_{3},\varepsilon) \tilde{G}_{i_{6}\gamma_{6},i_{3}\gamma_{3}}^{*aa^{*}}(-\mathbf{k}_{1} - \mathbf{k}_{2} + \mathbf{k}_{3},\varepsilon)] \times \\ \times \Gamma_{i_{5}\gamma_{5},i_{6}\gamma_{6}}^{(0)i_{7}\alpha_{7}}(-\mathbf{k}_{3}, -\mathbf{k}_{1} - \mathbf{k}_{2} + \mathbf{k}_{3}) \tilde{G}_{i_{7}\gamma_{7},i_{8}\gamma_{8}}^{uu}(\mathbf{k}_{1} + \mathbf{k}_{2},0) \Gamma_{i_{5}\alpha_{8}}^{i_{6}\alpha_{8}}(\mathbf{k}_{1},\mathbf{k}_{1} + \mathbf{k}_{2}).$$

$$(113)$$

In expressions (112) and (113),

$$\Gamma_{i_1\gamma_1,i_2\gamma_2}^{(0)i\alpha}(\mathbf{k}_1,\mathbf{k}_2) = \sum_{n_1,n_2} v'_{n_1i_1\gamma_1,n_2i_2\gamma_2}^{ni\alpha} \exp(i\mathbf{k}_1 \cdot (\mathbf{r}_{n_1i_1} - \mathbf{r}_{ni}) + i\mathbf{k}_2 \cdot (\mathbf{r}_{n_2i_2} - \mathbf{r}_{ni})). \quad (114)$$

The Fourier transform of the mass operator of the electron-electron interactions can be represented as

$$\tilde{\Sigma}_{\text{ee }i\gamma,i'\gamma'}(\mathbf{k},\varepsilon) = \tilde{\Sigma}_{\text{ee }i\gamma,i'\gamma'}^{(1)}(\mathbf{k},\varepsilon) + \tilde{\Sigma}_{\text{ee }i\gamma,i'\gamma'}^{(2)}(\mathbf{k},\varepsilon), \qquad (115)$$

$$\tilde{\Sigma}_{\text{ee }i\gamma,i'\gamma'}^{(1)}(\mathbf{k},\varepsilon) = -\frac{1}{2\pi i} \frac{1}{N} \times$$

$$\times \int_{-\infty}^{\infty} d\varepsilon' f(\varepsilon') \sum_{\mathbf{k}_{1}} \Gamma_{i\gamma,i'\gamma'}^{(0) \ i_{2}\gamma_{2},i_{1}\gamma_{1}} (-\mathbf{k} - \mathbf{k}_{1}, \mathbf{k}_{1}) (\tilde{G}_{i_{1}\gamma_{1},i_{2}\gamma_{2}}^{aa^{+}}(\mathbf{k}_{1},\varepsilon') - \tilde{G}_{i_{1}\gamma_{1},i_{2}\gamma_{2}}^{* \ aa^{+}}(\mathbf{k}_{1},\varepsilon')),$$
(116)

$$\tilde{\Sigma}_{\text{ee }i\gamma,i'\gamma'}^{(2)}(\mathbf{k},\varepsilon) = -\left(\frac{1}{2\pi iN}\right)^{2} \int_{-\infty}^{\infty} d\varepsilon_{1} \int_{-\infty}^{\infty} d\varepsilon_{2} f(\varepsilon_{1}) f(\varepsilon_{2}) \times \\
\times \sum_{\mathbf{k}_{1},\mathbf{k}_{2}} \Gamma_{i_{2}\gamma_{2},i_{1}\gamma_{1}}^{(0) i\gamma,i_{3}\gamma_{3}}(-\mathbf{k},-\mathbf{k}_{1}-\mathbf{k}_{2}+\mathbf{k},\mathbf{k}_{1}) [(\tilde{G}_{i_{2}\gamma_{2},i_{5}\gamma_{5}}^{aa^{+}}(\mathbf{k}-\mathbf{k}_{1}-\mathbf{k}_{2},\varepsilon-\varepsilon_{1}-\varepsilon_{2}) \times \\
\times \tilde{G}_{i_{1}\gamma_{1},i_{4}\gamma_{4}}^{*aa^{+}}(\mathbf{k}_{1},\varepsilon_{1}) - \tilde{G}_{i_{2}\gamma_{2},i_{5}\gamma_{5}}^{*aa^{+}}(\mathbf{k}-\mathbf{k}_{1}-\mathbf{k}_{2},\varepsilon-\varepsilon_{1}-\varepsilon_{2}) \tilde{G}_{i_{1}\gamma_{1},i_{4}\gamma_{4}}^{aa^{+}}(\mathbf{k}_{1},\varepsilon_{1})] \times \\
\times (\tilde{G}_{i_{6}\gamma_{6},i_{3}\gamma_{3}}^{aa^{+}}(\mathbf{k}_{2},\varepsilon_{2}) - \tilde{G}_{i_{6}\gamma_{6},i_{3}\gamma_{3}}^{*aa^{+}}(\mathbf{k}_{2},\varepsilon_{2})) - (\tilde{G}_{i_{2}\gamma_{2},i_{5}\gamma_{5}}^{aa^{+}}(\mathbf{k}-\mathbf{k}_{1}-\mathbf{k}_{2},\varepsilon-\varepsilon_{1}-\varepsilon_{2}) - \\
- \tilde{G}_{i_{2}\gamma_{2},i_{5}\gamma_{5}}^{*aa^{+}}(\mathbf{k}-\mathbf{k}_{1}-\mathbf{k}_{2},\varepsilon-\varepsilon_{1}-\varepsilon_{2}))(\tilde{G}_{i_{4}\gamma_{1},i_{4}\gamma_{4}}^{aa^{+}}(\mathbf{k}_{1},\varepsilon_{1})\tilde{G}_{i_{6}\gamma_{6},i_{3}\gamma_{3}}^{aa^{+}}(\mathbf{k}_{2},\varepsilon_{2})) - \\
- \tilde{G}_{i_{1}\gamma_{1},i_{4}\gamma_{4}}^{*aa^{+}}(\mathbf{k}_{1},\varepsilon_{1})\tilde{G}_{i_{6}\gamma_{6},i_{3}\gamma_{3}}^{*aa^{+}}(\mathbf{k}_{2},\varepsilon_{2}))]\Gamma_{i_{4}\gamma_{4},i_{7}'}^{i_{5}\gamma_{5},i_{6}\gamma_{6}}(\mathbf{k}-\mathbf{k}_{1}-\mathbf{k}_{2},\mathbf{k}_{2},\mathbf{k}_{1}).$$
(117)

The vertex part of the mass operator of the electron-electron interaction is determined by the equation

$$\begin{split} \Gamma^{i_{5}\gamma_{5},i_{6}\gamma_{6}}_{i_{4}\gamma_{4},i'\gamma'}(\mathbf{k}_{1},\mathbf{k}_{2},\mathbf{k}_{3}) &= \Gamma^{(0)}_{i_{5}\gamma_{5},i_{6}\gamma_{6}}(\mathbf{k}_{1},\mathbf{k}_{2},\mathbf{k}_{3}) - \frac{1}{2\pi i N} \int_{-\infty}^{\infty} d\varepsilon f(\varepsilon) \times \\ &\times \sum_{\mathbf{k}_{4}} \Gamma^{(0)}_{i_{5}\gamma_{5},i_{7}\gamma_{7}}(\mathbf{k}_{1},\mathbf{k}_{2},\mathbf{k}_{4}) [(\tilde{G}^{aa^{+}}_{i_{7}\gamma_{7},i_{9}\gamma_{9}}(\mathbf{k}_{4},\varepsilon) \tilde{G}^{*aa^{+}}_{i_{8}\gamma_{8},i_{10}\gamma_{10}}(-\mathbf{k}_{1}-\mathbf{k}_{2}-\mathbf{k}_{4},\varepsilon) - \\ &- \tilde{G}^{*aa^{+}}_{i_{7}\gamma_{7},i_{9}\gamma_{9}}(\mathbf{k}_{4},\varepsilon) \tilde{G}^{aa^{+}}_{i_{8}\gamma_{8},i_{10}\gamma_{10}}(-\mathbf{k}_{1}-\mathbf{k}_{2}-\mathbf{k}_{4},\varepsilon)] \Gamma^{i_{9}\gamma_{9},i_{6}\gamma_{6}}_{i_{10}\gamma_{10},i'\gamma'}(\mathbf{k}_{1}+\mathbf{k}_{2}+\mathbf{k}_{4},-\mathbf{k}_{4},\mathbf{k}_{3}). \end{split}$$

In expressions (116)–(118),

$$\Gamma_{i_{1}\gamma_{1},i_{7}}^{(0)}(\mathbf{k}_{1},\mathbf{k}_{2},\mathbf{k}_{3}) = \\ = \sum_{n_{1},n_{2},n_{3}} \tilde{v}_{n_{3}i_{3}\gamma_{3},n_{i_{7}}}^{(2)} n_{1}i_{1}\gamma_{1},n_{2}i_{2}\gamma_{2}} \exp(i\mathbf{k}_{1} \cdot (\mathbf{r}_{n_{1}i_{1}} - \mathbf{r}_{n_{i}}) + i\mathbf{k}_{2} \cdot (\mathbf{r}_{n_{2}i_{2}} - \mathbf{r}_{n_{i}}) + i\mathbf{k}_{3} \cdot (\mathbf{r}_{n_{3}i_{3}} - \mathbf{r}_{n_{i}})).$$
(119)

Green's functions $\tilde{G}^{aa^{\dagger}}(\mathbf{k}, \varepsilon)$, $\tilde{G}^{uu}(\mathbf{k}, \varepsilon)$, for the perfect crystal in formulae for mass operators $\tilde{\Sigma}_{\rm eph}(\mathbf{k}, \varepsilon)$, $\tilde{\Sigma}_{\rm ee}(\mathbf{k}, \varepsilon)$, $\tilde{\Sigma}_{\rm phe}(\mathbf{k}, \varepsilon)$, $\tilde{\Sigma}_{\rm phph}(\mathbf{k}, \varepsilon)$ are obtained from Eqs. (103)–(105), (107)–(119), if the coherent potentials within them are set equal to $\sigma(\mathbf{k}, \varepsilon) = i\delta$ (where $\delta \to +0$).

The solution of the set of Eqs. (103)–(105), (107)–(119) for the Green's functions of the subsystems of electrons and phonons, $\tilde{G}^{aa^{\dagger}}(\mathbf{k},\varepsilon)$, $\tilde{G}^{uu}(\mathbf{k},\varepsilon)$, can be performed *via* the iteration method.

The energies of electrons and phonons within the crystal are determined from the equations for the poles of the Green's functions of electrons and phonons, $\tilde{G}^{aa^+}(\mathbf{k}, \varepsilon)$, $\tilde{G}^{uu}(\mathbf{k}, \varepsilon)$:

$$\det \left\| \varepsilon \delta_{ii'} \delta_{\gamma \gamma'} - \tilde{H}_{i\gamma,i'\gamma'}(\mathbf{k}, \varepsilon) \right\| = 0, \tag{120}$$

$$\det \left\| \varepsilon^2 M_i \delta_{ii'} \delta_{\alpha \alpha'} / \hbar^2 - \tilde{\Phi}_{i\alpha,i'\alpha'}(\mathbf{k}, \varepsilon) \right\| = 0, \qquad (121)$$

where $\tilde{H}_{i_{\prime},i_{\prime}\prime}(\mathbf{k},\varepsilon)$, $\tilde{\Phi}_{i_{\alpha},i_{\alpha}\prime}(\mathbf{k},\varepsilon)$ are given by the formulae (104), (108).

Expressions for coherent potentials in formulae (105), (109) are obtained from condition (101) and have the forms

$$\sigma_{e}^{n_{1}i_{1}}(\varepsilon) = \langle (1 - (\Sigma_{e}^{n_{1}i_{1}} - \sigma_{e}^{n_{1}i_{1}}(\varepsilon))\tilde{G}^{aa^{+}}(\varepsilon))^{-1}\rangle^{-1} \times
\times \langle (1 - (\Sigma_{e}^{n_{1}i_{1}} - \sigma_{e}^{n_{1}i_{1}}(\varepsilon))\tilde{G}^{aa^{+}}(\varepsilon))^{-1}\Sigma_{e}^{n_{1}i_{1}}\rangle$$
(122)

$$\sigma_{\rm ph}^{n_1 i_1}(\varepsilon) = \langle (1 - (\Sigma_{\rm ph}^{n_1 i_1} - \sigma_{\rm ph}^{n_1 i_1}(\varepsilon)) \tilde{G}^{uu}(\varepsilon))^{-1} \rangle^{-1} \times \\
\times \langle (1 - (\Sigma_{\rm ph}^{n_1 i_1} - \sigma_{\rm ph}^{n_1 i_1}(\varepsilon)) \tilde{G}^{uu}(\varepsilon))^{-1} \Sigma_{\rm ph}^{n_1 i_1} \rangle$$
(123)

Thus, for the determination of the Green's functions of the effective medium, it is necessary to solve a set of Eqs. (102)–(119), (122), (123). Such a solution can be performed numerically by the iteration method. The calculation algorithm is described below in Sec. 8.

Using Eqs. (28) and (99), we deduce an expression for the self-energy, which describes the scattering of electrons:

$$\Sigma_{e \, ni\gamma, n'i'\gamma'}^{n_1i_1} = w_{ni\gamma, n'i'\gamma'}^{n_1i_1} = w_{ni\gamma, n'i'\gamma'}^{n_1i_2}. \tag{124}$$

Using Eqs. (58) and (100), we derive the initial expression for the self-energy, which describes the scattering of phonons:

$$\Sigma_{\text{ph }ni\alpha,n'i'\alpha'}^{n_1i_1}(\epsilon) = \frac{\hbar^2}{\epsilon^2} \sum_{\alpha_1} \Phi_{ni\alpha,n_1i_1\alpha_1}^{(0)} \left(\frac{1}{M_{n_1i_1}} - \frac{1}{M_{i_1}} \right) \Phi_{n_1i_1\alpha_1,n'i'\alpha'}^{(0)}.$$
 (125)

In the limit of an infinite crystal, all terms on the left sides of Eqs. (99), (100), except the first ones, tend to zero as 1/(vN) as the number vN of crystal sites (atoms) increases unrestrictedly.

Cluster decomposition for the Green's function of electrons and phonons of a disordered crystal can be obtained from Eqs. (95)–(101). The densities of electron and phonon states are presented as infinite series. Here, processes of scattering on clusters with different numbers of atoms are described by each term. As shown, the contribution of scattering processes of electrons and phonons on clusters decreases with increasing number of atoms in the cluster by a small parameter [33]

$$p(\varepsilon) = \frac{1}{r_{V}} \left| \sum_{(n_{2}i_{2})\neq(n_{1}i_{1}), i\gamma} \langle t^{n_{1}i_{1}}(\varepsilon)\tilde{G}(\varepsilon)t^{n_{2}i_{2}}(\varepsilon)\tilde{G}(\varepsilon) \rangle_{0i\gamma,0i\gamma} \right|, \qquad (126)$$

where r is the total number of energy bands included in the calculation. As shown previously [26, 30, 33], this parameter remains small when many parameters of the system are changed, except possibly for narrow energy intervals near the band edges.

By neglecting the contribution of processes of electron scattering on clusters consisting of three or more atoms, which is small by the above parameter, for the electron density of states, we obtain

$$g_{e}(\varepsilon) = \frac{1}{V} \sum_{i,\lambda,\gamma} P_{ii}^{\lambda} g_{\gamma}^{\lambda n i}(\varepsilon), \qquad (127)$$

where the conditional partial density of states is as follows:

$$g_{\gamma}^{\lambda ni}(\varepsilon) = -\frac{1}{\pi} \operatorname{Im} [\tilde{G} + \tilde{G} t^{\lambda ni} \tilde{G} + \sum_{(lj) \neq (ni), \lambda'} P_{lj \ ni}^{\lambda'/\lambda} \tilde{G} T^{(2) \ \lambda ni, \lambda' lj} \tilde{G}]_{ni\gamma, ni\gamma}, \quad (128)$$

$$T^{(2) \lambda n i, \lambda' l j} = [I - t^{\lambda n i} \tilde{G} t^{\lambda' l j} \tilde{G}]^{-1} t^{\lambda n i} \tilde{G} t^{\lambda' l j} [I + \tilde{G} t^{\lambda n i}], \qquad (129)$$

where $\tilde{G} = \tilde{G}^{aa^+}(\varepsilon)$.

The phonon density of states can be obtained similarly by averaging the phonon Green's function $G^{uu}(\varepsilon)$:

$$g_{\rm ph}(\varepsilon) = \frac{1}{V} \sum_{i,\lambda,\alpha} P_{ni}^{\lambda} g_{\alpha}^{\lambda ni}(\varepsilon) , \qquad (130)$$

$$g_{\alpha}^{\lambda ni}(\varepsilon) = -\frac{1}{\pi} \operatorname{Im} [\tilde{G} + \tilde{G} t^{\lambda ni} \tilde{G} + \sum_{(lj) \neq (ni), \lambda'} P_{lj \ ni}^{\lambda'/\lambda} \tilde{G} T^{(2) \ \lambda ni, \lambda' lj} \tilde{G}]_{ni\alpha, ni\alpha}, \quad (131)$$

where $\tilde{G} = \tilde{G}^{uu}(\varepsilon)$.

In Eqs. (128) and (131), $P_{lj\;nl}^{\lambda'/\lambda}$ is the conditional probability to find an atom of the λ' sort at the site (lj) with number of electrons per atom equal to $Z_{\lambda'}$ and a magnetic moment equal to $m_{\lambda'}$, provided that, at the site (ni), an atom of the λ sort is located with number of electrons per atom equal to Z_{λ} and a magnetic moment equal m_{λ} . Here, $t^{\lambda nl}$ is the value of the matrix element of a single-centre operator for scattering in the case where an

atom of the λ sort is located at the site (*ni*) and has a number of electrons per atom equal to Z_{λ} and a magnetic moment equal to m_{λ} .

When the system is disordered, we need to consider a random arrangement of the atoms on lattice sites. Hence, in Eqs. (127) and (130), the probability for an atom of the λ sort to be at the site (0*i*) is given by the following definition:

$$P_{ni}^{\lambda} = \langle c_{ni}^{\lambda} \rangle , \qquad (132)$$

where c_{ni}^{λ} is a discrete binary random number taking the values of 1 or 0 depending on whether an atom of the λ sort is located at the site (ni) or not. The conditional probabilities in Eqs. (127) and (128), as well as in (130) and (131) are defined by the following equation:

$$P_{lj\ ni}^{\lambda'\lambda} = P_{ni}^{\lambda} P_{lj\ ni}^{\lambda'/\lambda} = \langle c_{lj}^{\lambda'} c_{ni}^{\lambda} \rangle. \tag{133}$$

The notations P_{ni}^{λ} and $P_{lj\;ni}^{\lambda'/\lambda}$ determine the probabilities of the fluctuations of concentration, electron density, and spin density.

6. Free Energy

We first focus on the Gibbs free energy (also called the thermodynamic potential) of the system, which satisfies the definition [33]:

$$\Omega = -\Theta \ln \operatorname{Tr}(e^{-H/\Theta}). \tag{134}$$

The Hamiltonian H is defined in Eq. (1). To perform the trace operation, we need to sum over all the band states, but we also need to consider the disorder averaging. The latter is commonly handled via a configurational average [33]. Using formulae (50) and (134), we represent the thermodynamic potential in the form

$$\Omega = \Omega_{\rm e}^{(0)} + \Omega_{\rm ph}^{(0)} + \Omega', \qquad (135)$$

where $\Omega_{\rm e}^{(0)}$ and $\Omega_{\rm ph}^{(0)}$ are the thermodynamic potentials for the electrons and the phonons, respectively. The symbol Ω' denotes the contribution to the thermodynamic potential, which is determined by the mutual scattering of electrons and phonons; it is defined as

$$\Omega' = -\Theta \ln(\langle \sigma(1/\Theta) \rangle_0) \tag{136}$$

with σ given in Eq. (50).

Next, we use the method of 'integration over the coupling constant' to simplify the results further.

By replacing the interacting Hamiltonian $H_{\rm int}$ (defined in Eq. (5)) by $H_{\rm int}(\lambda) = \lambda H_{\rm int}$, differentiating the expression for the piece of thermodynamic potential $\Omega'(\lambda)$ in Eq. (136) concerning parameter λ , and then integrating (with the boundary conditions $\Omega'(0) = 0$ and $\Omega'(1) = \Omega'$), we obtain the following expression [33]:

$$\Omega' = \Theta \int_{0}^{1} \frac{d\lambda}{\lambda} \int_{0}^{1/\Theta} d\tau \langle T_{\tau} H_{\text{int}}(\tau, \lambda) \sigma(1/\Theta, \lambda) \rangle_{0} / \langle \sigma(1/\Theta, \lambda) \rangle_{0}.$$
 (137)

Using the diagram technique described in Ref. [30], we reduce Eq. (137) to the form

$$\Omega' = -\frac{1}{\pi \nu N} \operatorname{Im} \int_{0}^{1} \frac{d\lambda}{\lambda} \int_{-\infty}^{\infty} d\varepsilon [f(\varepsilon) \operatorname{Tr} \langle (w(\lambda) + \Sigma_{\text{eph}}(\varepsilon, \lambda) + \Sigma_{\text{ee}}(\varepsilon, \lambda)) G^{aa^{+}}(\varepsilon, \lambda) \rangle + \frac{1}{2} \operatorname{cth} \left(\frac{\varepsilon}{2\Theta} \right) \operatorname{Tr} \langle (\Sigma_{M}(\varepsilon, \lambda) + \Delta \Phi(\lambda) + \Sigma_{\text{phe}}(\varepsilon, \lambda) + \Sigma_{\text{phph}}(\varepsilon, \lambda)) G^{uu}(\varepsilon, \lambda) \rangle].$$
(138)

This expression can be immediately evaluated, because we know all the Green's functions and the self-energies.

The contribution to the thermodynamic potential from the electrons (in the atomic-nuclei field) is simple to find too; it is given by

$$\Omega_{\rm e}^{(0)} = -\Theta \int_{-\infty}^{\infty} d\varepsilon g_{\rm e}^{(0)}(\varepsilon) \ln(1 + e^{(\mu - \varepsilon)/\Theta}). \tag{139}$$

Similarly, the contribution to the thermodynamic potential from the phonons is given by

$$\Omega_{\rm ph}^{(0)} = \Theta \int_{-\infty}^{\infty} d\varepsilon g_{\rm ph}^{(0)}(\varepsilon) \ln(1 - e^{-\varepsilon/\Theta}). \tag{140}$$

The values $g_e^{(0)}(\varepsilon)$ and $g_{ph}^{(0)}(\varepsilon)$ in Eqs. (139) and (140) are given by formulae (127) and (130), where $t^{\lambda nl} = 0$.

Expanding the Green's function $G^{aa^+}(\varepsilon,\lambda)$ and $G^{uu}(\varepsilon,\lambda)$ in Eq. (138) into a power series (see (56), (57)), calculating the energy integral by integration by parts, performing cyclic permutations of the operators under sign Tr, and substituting expression (138) for Ω' into formula (135), we obtain the expression

$$\Omega = \Omega_{\rm e} + \Omega_{\rm ph}, \tag{141}$$

where $\Omega_{\rm e}$ and $\Omega_{\rm ph}$ are given by Eqs. (139) and (140), but with $g_{\rm e}^{(0)}$ and $g_{\rm ph}^{(0)}$ replaced by $g_{\rm e}(\epsilon)$ and $g_{\rm ph}(\epsilon)$ (see Eqs. (127) and (130)).

Ultimately, we are interested in determining the Helmholtz free energy F as a function of the volume (V), the temperature (T), and the number of electrons (N_e) ; it can be found directly from the thermodynamic potential, inasmuch as it satisfies the relation $F = \Omega + \mu \langle N_e \rangle$. This free energy per atom can be presented [33] as

$$F = \Omega_e + \Omega_{\rm ph} + \mu \langle Z \rangle . \tag{142}$$

The equilibrium values of the parameters of interatomic correlations, P_{ni}^{λ} and $P_{lj\,ni}^{\lambda'/\lambda}$, in Eqs. (127), (128), (130), (131) and of the static displacements of the atomic nuclei can be found from the condition for the minimum free energy F. Fourier components $P_{ji}^{\lambda'/\lambda}(\mathbf{k})$ of quantities $P_{lj\,ni}^{\lambda'/\lambda}$ describe static waves of concentrations, electron density, spin density, and nuclei displacements, which, for one's turn, describe the phase state of a disordered crystal.

7. Electrical Conductivity

In this section, we discuss how to calculate the electrical conductivity. We assume that the system will not be driven too far from equilibrium. Accordingly, we use the Kubo linear-response formalism for the electrical-conductivity tensor [30], which is given by

$$\sigma_{\alpha\beta}(\omega) = \int_{0}^{1/\Theta} \int_{0}^{\infty} d\tau dt e^{i\omega t - \delta t} \langle J_{\beta}(0) J_{\alpha}(t + i\hbar\tau) \rangle.$$
 (143)

In this equation, J_{α} is the current operator along the α -th spatial direction; ω is a frequency of the external electric field $\mathbf{E}(\omega, \delta)$, and an infinitely small positive quantity δ is a time increment of its increase during (adiabatic) switching on $(\delta \to +0)$. The real part of the conductivity, called the optical conductivity, can be represented in terms of the imaginary part of the retarded response function or equivalently as

$$\operatorname{Re} \sigma_{\alpha\beta}(\omega) = \frac{i}{2\omega} (G_{\mathbf{r}}^{J_{\alpha}J_{\beta}}(\omega) - G_{\mathbf{a}}^{J_{\alpha}J_{\beta}}(\omega))$$
 (144)

in terms of the retarded and advanced response functions.

The current operator is just the number operator for the electrons, which is multiplied by their velocity and the electric charge, and then summed over all states. It can be compactly represented as

$$J_{\alpha}(t) = e \int d\xi \Psi^{+}(\xi, t) \nu_{\alpha} \Psi(\xi, t) , \qquad (145)$$

where $\Psi^+(\xi, t)$ and $\Psi(\xi, t)$ are the field operators for the creation and destruction of electrons, respectively, v_{α} is the operator of α component of the band velocity, and e is the electron charge.

The integration over ξ in Eq. (145) runs over all states. (Especially, by integration over ξ we mean integration within the unit volume of the crystal and summation over the projections of the spin σ onto the Oz axis.)

To calculate the two-time Green's functions, which are used to determine the electrical conductivity of a crystal, the temperature Green's function and the known relationship between the spectral representations of the two-time Green's function and the temperature Green's function are used.

In this case, the temperature Green's function is

$$G^{J_{\alpha}J_{\beta}}(\tau,\tau') = \frac{e^2}{NV_1} \sum_{n_1 n_2 n_3 n_4} v_{\alpha n_4 n_2} v_{\beta n_3 n_1} G''(n_1 \tau', n_2 \tau, n_3 \tau', n_4 \tau), \qquad (146)$$

where V_1 is the volume of the primitive unit cell, and the two-particle temperature Green's function is given by the following expression:

$$G''(n_1\tau',n_2\tau,n_3\tau',n_4\tau) = \langle T_{\tau}a_{n_1}(\tau')a_{n_2}(\tau)a_{n_3}^+(\tau')a_{n_4}^+(\tau)\sigma(1/\Theta)\rangle_0 \langle \sigma(1/\Theta)\rangle_0 \quad (147)$$

 $(n \triangleq (ni\gamma))$. Thus, the two-particle temperature Green's function is expressed as a series of connected diagrams. It is described by the

Fig. 6. Diagrams for the two-particle Green's

the right side of the equation in Fig. 6 are the same as those in Fig. 4.) The

numbers in Fig. 6 correspond to the number of a point on the diagram. For example, the number 1 corresponds to $(n_1i_1\gamma_1\tau_1)$.

The temperature two-particle Green's function, which determines the electrical conductivity of the crystal, is described only by the first and third diagrams on the right-hand side of the equation in Fig. 6. This follows from Eq. (145) for the current-density operator, which is expressed through the product of the electron creation and destruction operators. This temperature Green's function differs from the Green's function in quantum field theory [37], which is described by all three diagrams on the right-hand side of the equation in Fig. 6.

Using the diagram technique for the temperature Green's function and neglecting the contributions of scattering processes on clusters of three or more sites to the electrical-conductivity tensor, we obtain:

$$\begin{split} \operatorname{Re}\,\sigma_{\alpha\beta}(\omega) &= \frac{e^2\hbar}{4\pi V_1\epsilon} \{\int\limits_{-\infty}^{\infty} d\epsilon_1 (f(\epsilon_1+\epsilon)-f(\epsilon_1)) \sum\limits_{s,s'=+,-} (2\delta_{ss'}-1) \times \\ &\sum\limits_{i\gamma} \{v_{\beta}\tilde{K}(\epsilon_1^s,v_{\alpha},\epsilon_1^{s'}+\epsilon) + \sum\limits_{\lambda} P_{ni}^{\lambda}\tilde{K}(\epsilon_1^{s'}+\epsilon,v_{\beta},\epsilon_1^s)t^{\lambda ni}(\epsilon_1^s)\tilde{K}(\epsilon_1^s,v_{\alpha},\epsilon_1^{s'}+\epsilon) \times \\ &\times t^{\lambda ni}(\epsilon_1^{s'}+\epsilon) + \sum\limits_{\lambda} P_{ni}^{\lambda} \sum\limits_{lj\neq ni,\,\lambda'} P_{lj}^{\lambda'/\lambda} [\tilde{K}(\epsilon_1^{s'}+\epsilon,v_{\beta},\epsilon_1^s)v_{\alpha}\tilde{G}(\epsilon_1^{s'}+\epsilon)T^{(2)\lambda ni,\lambda' lj}(\epsilon_1^{s'}+\epsilon) + \\ &+ \tilde{K}(\epsilon_1^s,v_{\alpha},\epsilon_1^{s'}+\epsilon)v_{\beta}\tilde{G}(\epsilon_1^s)T^{(2)\lambda ni,\lambda' lj}(\epsilon_1^s) + \tilde{K}(\epsilon_1^{s'}+\epsilon,v_{\beta},\epsilon_1^s)[t^{\lambda' lj}(\epsilon_1^s) \times \\ &\times \tilde{K}(\epsilon_1^s,v_{\alpha},\epsilon_1^{s'}+\epsilon)t^{\lambda ni}(\epsilon_1^{s'}+\epsilon) + (t^{\lambda ni}(\epsilon_1^s)+t^{\lambda' lj}(\epsilon_1^s))\tilde{K}(\epsilon_1^s,v_{\alpha},\epsilon_1^{s'}+\epsilon) \times \\ &\times T^{(2)\lambda ni,\lambda' lj}(\epsilon_1^{s'}+\epsilon) + T^{(2)\lambda' lj,\lambda ni}(\epsilon_1^s)\tilde{K}(\epsilon_1^s,v_{\alpha},\epsilon_1^{s'}+\epsilon)(t^{\lambda ni}(\epsilon_1^{s'}+\epsilon)+t^{\lambda' lj}(\epsilon_1^{s'}+\epsilon)) + \\ &+ T^{(2)\lambda' lj,\lambda ni}(\epsilon_1^s)\tilde{K}(\epsilon_1^s,v_{\alpha},\epsilon_1^{s'}+\epsilon)T^{(2)\lambda ni,\lambda' lj}(\epsilon_1^{s'}+\epsilon) + T^{(2)\lambda' lj,\lambda ni}(\epsilon_1^s)\tilde{K}(\epsilon_1^s,v_{\alpha},\epsilon_1^{s'}+\epsilon) \times \\ &\times T^{(2)\lambda' lj,\lambda ni}(\epsilon_1^{s'}+\epsilon) \|\}_{ni\gamma,ni\gamma} + \int\limits_{-\infty}^{\infty}\int\limits_{-\infty}^{\infty} d\epsilon_1 d\epsilon_2 f(\epsilon_1) f(\epsilon_2) \Delta G_{\alpha\beta}^{\Pi}(\epsilon_1,\epsilon_2;\epsilon) \}, \end{split}$$

where

$$\tilde{K}(\varepsilon_1^s, \nu_\alpha, \varepsilon_1^{s'} + \varepsilon) = \tilde{G}^{aa^+}(\varepsilon_1^{s'})\nu_\alpha \tilde{G}^{aa^+}(\varepsilon_1^{s'} + \varepsilon), \qquad (149)$$

$$\tilde{G}^{aa^+}(\varepsilon_1^+) = \tilde{G}_r^{aa^+}(\varepsilon_1), \qquad (150)$$

$$\tilde{G}^{aa^{+}}(\varepsilon_{1}^{-}) = \tilde{G}_{a}^{aa^{+}}(\varepsilon_{1}) = \tilde{G}_{r}^{*aa^{+}}(\varepsilon_{1}). \tag{151}$$

The two-particle interaction term $\Delta G_{\alpha\beta}^{II}(\epsilon_1, \epsilon_2; \epsilon)$ in (148) is

$$\begin{split} \Delta G^{\mathrm{II}}_{\alpha\beta}(\epsilon_{1},\epsilon_{2};\epsilon) &= \frac{i v_{\alpha n_{4} n_{2}} v_{\beta n_{3} n_{1}}}{2\pi N} \{ (\tilde{G}^{aa^{+}}_{rn_{1} n_{6}}(\epsilon_{1}) - \tilde{G}^{aa^{+}}_{an_{1} n_{6}}(\epsilon_{1})) (\tilde{G}^{aa^{+}}_{rn_{2} n_{5}}(\epsilon_{2}) - \tilde{G}^{aa^{+}}_{an_{2} n_{5}}(\epsilon_{2})) \times \\ &\times (\tilde{G}^{aa^{+}}_{an_{7} n_{4}}(\epsilon_{2} - \epsilon) \tilde{G}^{aa^{+}}_{rn_{8} n_{3}}(\epsilon_{1} + \epsilon) - \tilde{G}^{aa^{+}}_{rn_{7} n_{4}}(\epsilon_{2} - \epsilon) \tilde{G}^{aa^{+}}_{an_{8} n_{3}}(\epsilon_{1} + \epsilon)) + \tilde{G}^{aa^{+}}_{an_{1} n_{6}}(\epsilon_{1} - \epsilon) \times \\ &\times (\tilde{G}^{aa^{+}}_{rn_{2} n_{5}}(\epsilon_{2}) - \tilde{G}^{aa^{+}}_{an_{2} n_{5}}(\epsilon_{2})) \tilde{G}^{aa^{+}}_{an_{7} n_{4}}(\epsilon_{2} - \epsilon) (\tilde{G}^{aa^{+}}_{rn_{8} n_{3}}(\epsilon_{1}) - \tilde{G}^{aa^{+}}_{an_{8} n_{3}}(\epsilon_{1})) - \tilde{G}^{aa^{+}}_{rn_{1} n_{6}}(\epsilon_{1} - \epsilon) \times \\ &\times (\tilde{G}^{aa^{+}}_{rn_{2} n_{5}}(\epsilon_{2}) - \tilde{G}^{aa^{+}}_{an_{2} n_{5}}(\epsilon_{2})) \tilde{G}^{aa^{+}}_{an_{7} n_{4}}(\epsilon_{2} - \epsilon) (\tilde{G}^{aa^{+}}_{rn_{8} n_{3}}(\epsilon_{1}) - \tilde{G}^{aa^{+}}_{an_{8} n_{3}}(\epsilon_{1})) + (\tilde{G}^{aa^{+}}_{an_{1} n_{6}}(\epsilon_{1} - \epsilon) \times \\ &\times (\tilde{G}^{aa^{+}}_{rn_{2} n_{5}}(\epsilon_{2}) - \tilde{G}^{aa^{+}}_{an_{2} n_{5}}(\epsilon_{2})) \tilde{G}^{aa^{+}}_{rn_{7} n_{4}}(\epsilon_{2} - \epsilon) (\tilde{G}^{aa^{+}}_{rn_{8} n_{3}}(\epsilon_{1}) - \tilde{G}^{aa^{+}}_{an_{8} n_{3}}(\epsilon_{1})) + (\tilde{G}^{aa^{+}}_{an_{1} n_{6}}(\epsilon_{1} - \epsilon) \times \\ &\times (\tilde{G}^{aa^{+}}_{rn_{2} n_{5}}(\epsilon_{2}) - \tilde{G}^{aa^{+}}_{an_{2} n_{5}}(\epsilon_{2}) - \tilde{G}^{aa^{+}}_{an_{7} n_{4}}(\epsilon_{2}) - \tilde{G}^{aa^{+}}_{an_{7} n_{4}}(\epsilon_{2})) (\tilde{G}^{aa^{+}}_{rn_{8} n_{3}}(\epsilon_{1}) - \tilde{G}^{aa^{+}}_{an_{8} n_{3}}(\epsilon_{1})) + (\tilde{G}^{aa^{+}}_{rn_{7} n_{6}}(\epsilon_{1}) - \tilde{G}^{aa^{+}}_{an_{1} n_{6}}(\epsilon_{1})) \tilde{G}^{aa^{+}}_{rn_{2} n_{5}}(\epsilon_{2} + \epsilon) (\tilde{G}^{aa^{+}}_{rn_{7} n_{4}}(\epsilon_{2}) - \tilde{G}^{aa^{+}}_{an_{7} n_{4}}(\epsilon_{2})) \times \\ &\times (\tilde{G}^{aa^{+}}_{rn_{8} n_{3}}(\epsilon_{1}) + \epsilon) - (\tilde{G}^{aa^{+}}_{rn_{1} n_{6}}(\epsilon_{1}) - \tilde{G}^{aa^{+}}_{an_{1} n_{6}}(\epsilon_{1})) \tilde{G}^{aa^{+}}_{an_{2} n_{5}}(\epsilon_{2} + \epsilon) (\tilde{G}^{aa^{+}}_{rn_{7} n_{4}}(\epsilon_{2}) - \tilde{G}^{aa^{+}}_{an_{7} n_{4}}(\epsilon_{2})) \times \\ &\times (\tilde{G}^{aa^{+}}_{rn_{8} n_{3}}(\epsilon_{1}) + \epsilon) - (\tilde{G}^{aa^{+}}_{rn_{1} n_{6}}(\epsilon_{1}) - \tilde{G}^{aa^{+}}_{an_{1} n_{6}}(\epsilon_{1})) \tilde{G}^{aa^{+}}_{an_{2} n_{5}}(\epsilon_{2}) - \tilde{G}^{aa^{+}}_{an_{7} n_{4}}(\epsilon_$$

Summation over repeated indices in Eq. (152) is implied. The number N in Eq. (152) is reduced, when summing over the primitive unit-cell number n_1 , since the sum over the remaining indices does not depend on the primitive unit-cell number n_1 .

For the static conductivity tensor ($\omega \to 0$), we obtain

$$\begin{split} \sigma_{\alpha\beta} &= \frac{e^{2}\hbar}{4\pi V_{1}} \int_{-\infty}^{\infty} d\varepsilon_{1} \left(\frac{\partial f}{\partial \varepsilon_{1}} \right)_{s,s'=+,-} (2\delta_{ss'} - 1) \sum_{i\gamma} \{ \upsilon_{\beta} \tilde{K}(\varepsilon_{1}^{s}, \upsilon_{\alpha}, \varepsilon_{1}^{s'}) + \sum_{\lambda} P_{ni}^{\lambda} \tilde{K}(\varepsilon_{1}^{s'}, \upsilon_{\beta}, \varepsilon_{1}^{s}) \times \\ &\times t^{\lambda ni}(\varepsilon_{1}^{s}) \tilde{K}(\varepsilon_{1}^{s}, \upsilon_{\alpha}, \varepsilon_{1}^{s'}) t^{\lambda ni}(\varepsilon_{1}^{s'}) + \sum_{\lambda} P_{ni}^{\lambda} \sum_{lj \neq ni, \lambda'} P_{lj \ ni}^{\lambda'/\lambda} [\tilde{K}(\varepsilon_{1}^{s'}, \upsilon_{\beta}, \varepsilon_{1}^{s}) \upsilon_{\alpha} \tilde{G}(\varepsilon_{1}^{s'}) \times \\ &\times T^{(2)\lambda ni, \lambda' lj}(\varepsilon_{1}^{s'}) + \tilde{K}(\varepsilon_{1}^{s}, \upsilon_{\alpha}, \varepsilon_{1}^{s'}) \upsilon_{\beta} \tilde{G}(\varepsilon_{1}^{s}) T^{(2)\lambda ni, \lambda' lj}(\varepsilon_{1}^{s}) + \tilde{K}(\varepsilon_{1}^{s'}, \upsilon_{\beta}, \varepsilon_{1}^{s}) [t^{\lambda' lj}(\varepsilon_{1}^{s}) \times \\ &\times \tilde{K}(\varepsilon_{1}^{s}, \upsilon_{\alpha}, \varepsilon_{1}^{s'}) t^{\lambda ni}(\varepsilon_{1}^{s'}) + (t^{\lambda ni}(\varepsilon_{1}^{s}) + t^{\lambda' lj}(\varepsilon_{1}^{s})) \tilde{K}(\varepsilon_{1}^{s}, \upsilon_{\alpha}, \varepsilon_{1}^{s'}) T^{(2)\lambda ni, \lambda' lj}(\varepsilon_{1}^{s'}) + \\ &+ T^{(2)\lambda' lj, \lambda ni}(\varepsilon_{1}^{s}) \tilde{K}(\varepsilon_{1}^{s}, \upsilon_{\alpha}, \varepsilon_{1}^{s'}) (t^{\lambda ni}(\varepsilon_{1}^{s'}) + t^{\lambda' lj}(\varepsilon_{1}^{s'})) + T^{(2)\lambda' lj, \lambda ni}(\varepsilon_{1}^{s}) \tilde{K}(\varepsilon_{1}^{s}, \upsilon_{\alpha}, \varepsilon_{1}^{s'}) \times \\ &\times T^{(2)\lambda ni, \lambda' lj}(\varepsilon_{1}^{s'}) + T^{(2)\lambda' lj, \lambda ni}(\varepsilon_{1}^{s'}) \tilde{K}(\varepsilon_{1}^{s}, \upsilon_{\alpha}, \varepsilon_{1}^{s'}) T^{(2)\lambda' lj, \lambda ni}(\varepsilon_{1}^{s'}) \right]_{hiv, niv}. \end{split}$$

The electron velocity satisfies the conventional definition

$$v_{\alpha}(\mathbf{k}) = \frac{1}{\hbar} \frac{\partial H_0^{(1)}(\mathbf{k})}{\partial k_{\alpha}}.$$
 (154)

Under the deriving expression (153), the last small term resulting from the two-particle interaction in the expression for electrical conductivity (148) is neglected.

The method developed in this work was applied in Ref. [31] to study the effect of an impurity on the energy spectrum and electrical conductivity of carbon nanotubes.

In conclusion to this section, note that the Kubo formalism, or more precisely, Kubo-Greenwood (KG) formalism, is a reasonably efficient but effortful method widely used in the literature for its implementa-

tion in the numerical computations of electron diffusivity and conductivity. Among a series of numerical methods reported in the literature on studying the electronic and transport properties of single- and multilayer graphene films, the time-dependent real-space KG formalism has a linear dependence of computational capabilities on the size of a system and, therefore, has an advantage over some other methods in the investigation of realistically large graphene sheets containing millions of atoms. The KG-formalism-based computational methodology, applied for numerical calculation of the electron density of states, electron diffusivity and conductivity, is described in a series of works; see, e.g., review articles [39, 40] and chapters in the monographs [41-43] as well as references therein. This methodology includes the Chebyshov method for the solution of the time-dependent Schrödinger equation, calculation of the first diagonal element of the Green's function using the continued-fraction technique and tridiagonalization procedure for the Hamiltonian matrix, averaging over realizations of point [44-49] or extended (acting as the line scatterers) [50-53] or point + line [52, 53] defects, sizes of initial electron wave packet and computational domain, boundary conditions, etc.

8. Algorithm for Implementation of the Green's Function Method

As noted above, the phase state of a disordered crystal is generally described by static waves of concentrations, charge density, and spin density. The state of a crystal is determined by the symmetry of the crystal lattice and the parameters of correlations in the distribution of impurities, the number of electrons, and localized magnetic moments at the sites of the crystal lattice, which are found from the free energy minimum condition and depend on the chemical composition and external parameters, temperature, and pressure. Let us assume that we know the crystal symmetry characteristics, the value of which can be refined using the free energy minimum condition.

Thus, we set the main translation vectors of the crystal lattice $\{a_{\nu}\}$ and the position vectors of sublattice basis sites in the unit cell of the crystal $\{\rho_{i}\}$ (see Eq. (14)).

We set the values of concentrations c^{λ} and parameters of interatomic correlations in a disordered crystal P_{ni}^{λ} , $P_{lj\,ni}^{\lambda/\lambda}$ (see Eqs. (127), (128), (130), (131)), taking into account that

$$c^{\lambda} = v^{-1} \sum_{i=1}^{\nu} P_{ni}^{\lambda} , \qquad (155)$$

where v is the number of atoms per primitive unit cell.

Next, the values of the masses and charges of the nuclei of the crystal atoms are specified.

The next step in the numerical implementation of the method is the diagonalization of the basis in accordance with formulae (15)-(24). To do

this, it is necessary to calculate the Fourier components $S_{i_1\delta_1,i_2\delta_2}(\mathbf{k})$ of the overlap matrix using Eq. (16). Note that the value of $S_{i_1\delta_1,i_2\delta_2}(\mathbf{k})$ does not depend on the unit-cell number n_1 . The value of n_1 can be set as equal to $n_1=0$; when summing over n_2 , it can be limited to the sites (n_2i_2) of the lattice, which lie in the region of overlap of the wave functions of an electron in the field of nuclei located at the sites $(0i_1)$, (n_2i_2) . According to Eq. (14), summation over n_2 means summation over $l_v^{(2)}=...,-L/2$, -L/2+1,...,L/2-1, where L is an even integer. The number of primitive unit cells in a crystal is $N=L^3$, L^2 , L for three-dimensional, two-dimensional and one-dimensional crystals, respectively.

Using the values of the matrix elements $S_{i_1\delta_1,i_2\delta_2}(\mathbf{k})$, we find the matrix $S_{i_1\delta_1,i_2\delta_2}^{-1/2}(\mathbf{k})$. Then, using formula (24), orthogonal functions (15) are calculated. Further, the Fourier components $h_{i\gamma,i'\gamma}^{(0)}(\mathbf{k})$ of the hopping integrals are calculated using formula (25).

The initial values of the vertex parts of the electron-phonon and electron-electron interactions' mass operators $\Gamma^{(0)\,i'\alpha'}_{i_1\gamma_1,i_2\gamma_2}(\mathbf{k}_1,\mathbf{k}_2)$ and $\Gamma^{(0)\,i_5\gamma_5,i_6\gamma_6}_{i_4\gamma_4,i'\gamma'}(\mathbf{k}_1,\mathbf{k}_2,\mathbf{k}_3)$ are calculated using Eqs. (114) and (34) along with (119), (38), and (76).

The initial values of the Green's functions of the subsystems of electrons and phonons, $\tilde{G}^{aa^+}(\mathbf{k},\varepsilon)$ and $\tilde{G}^{uu^+}(\mathbf{k},\varepsilon)$, are calculated using Eqs. (103)–(105) and (107)–(110), in which the values of the mass operators of the electron–phonon, electron–electron, and phonon–electron interactions are assumed to be equal to zero.

We set the initial value of the Fermi level μ equal to the lowest energy value for the electron state within the nuclei field (see formula (27)).

Let us set the temperature value T.

We create the calculation cycle (i)-(vi) as follows.

- (i) The mass operators of the electron-phonon, phonon-electron and electron-electron interactions are calculated using formulae (111)-(119).
- (ii) The Green's functions for the subsystems of electrons and phonons, $\tilde{G}^{aa^{\dagger}}(\mathbf{k},\varepsilon)$ and $\tilde{G}^{uu^{\dagger}}(\mathbf{k},\varepsilon)$, are calculated using formulae (103)–(105) and (107)–(110).
- (iii) The coherent potentials for the subsystems of electrons and phonons, $\sigma_e^i(\varepsilon)$ and $\sigma_{ph}^i(\varepsilon)$, are calculated by formulae (122) and (123).
- (iv) The electron and phonon densities of states are calculated using formulae (127)–(131). During the matrix multiplication, summation by the matrix-elements' indices is performed following the formula (102):

$$\tilde{G}_{n_{3}i_{3}\gamma_{3},n_{4}i_{4}\gamma_{4}}^{aa^{+}}(\varepsilon) = \frac{1}{N} \sum_{\mathbf{k}} \tilde{G}_{i_{3}\gamma_{3},i_{4}\gamma_{4}}^{aa^{+}}(\mathbf{k},\varepsilon) \exp(i\mathbf{k} \cdot (\mathbf{r}_{n_{3}i_{3}} - \mathbf{r}_{n_{4}i_{4}})).$$
 (156)

- (v) The Fermi level μ is calculated *via* formulae (83)–(85).
- (vi) If the specified calculation accuracy is reached, the loop exits. Next, we calculate the value of free energy F using formula (142).

The above calculations will be performed for different values of the parameters of interatomic correlations, P_{ni}^{λ} and $P_{lj\,ni}^{\lambda'/\lambda}$, in Eqs. (127), (128), (130), (131), and for different values of the parameters of static displacements of the atomic nuclei. The values of these parameters for the thermodynamic-equilibrium state are found from the condition for the minimum of free energy F (142).

Further, using formulae (148), (153), both the high-frequency (optical) electrical conductivity and the static electrical conductivity are calculated.

Localized magnetic moments and ion charges are calculated using formulae (86), (88)–(91), and (128).

9. Energy Spectrum of Graphene with Adsorbed Potassium Atoms

To calculate the electron energy spectrum of graphene with adsorbed potassium atoms, we chose the wave functions of the 2s- and 2p-states of noninteracting neutral carbon atoms as the basis. In the calculation of matrix elements of the Hamiltonian, we take the first three coordination spheres. The energy spectrum of graphene is calculated for the temperature T=0 K. In calculations, we neglect the renormalization of the vertices of the mass operator of electron-electron interactions. The dependence of the energy of an electron on the wave vector for graphene is calculated from the equation for the Green's function poles for the electrons' subsystem, defined in Eq. (120).

Figure 7, left, [54] shows the dependence of the electron energy ε for the graphene with adsorbed potassium atoms on the wave vector \mathbf{k} . The vector \mathbf{k} is directed from the Brillouin-zone centre (point Γ) to the Dirac point (point K).

The structural periodic distance from a potassium atom to a carbon atom is 0.28 nm. It is seen in Fig. 7 that, at such an ordered arrangement of potassium atoms, a gap in the energy spectrum of graphene arises. Its value depends on the concentration of adsorbed potassium atoms, their location in the primitive unit cell, and the distance to carbon atoms. We revealed that, at the potassium concentration such that the primitive unit cell includes two carbon atoms and one potassium atom, if the latter is placed on the graphene-layer surface above a carbon atom at a distance of 0.286 nm, the energy gap is $\cong 0.25$ eV (see Fig. 7, right). The location of the Fermi level in the energy spectrum depends on the potassium concentration, and it is within the energy interval -0.36 Ry $\leq \varepsilon_r \leq -0.23$ Ry.

The band-gap value obtained in Ref. [54] well correlates with that calculated in Refs. [55, 56] for the ordered distribution of potassium adatoms residing on three types of high-symmetry positions ('hollow', 'bridge', or 'top' sites) over the graphene crystal lattice, where the authors of Refs. [55, 56] also applied the Green's function technique combined with a series

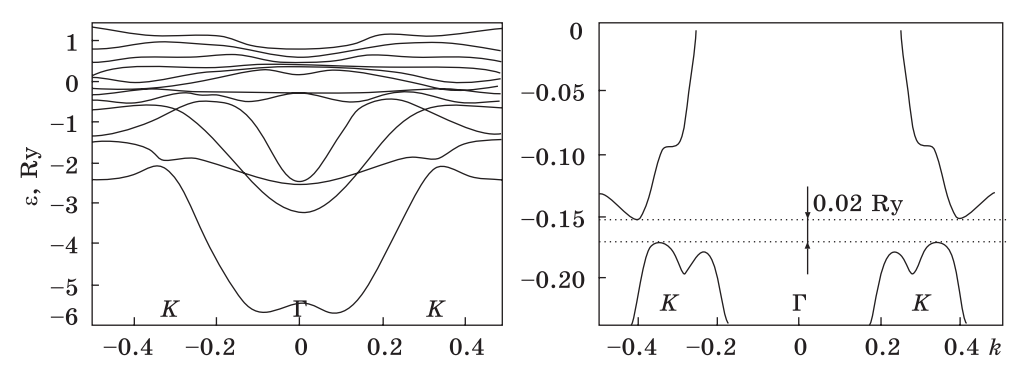


Fig. 7. Dependence of the electron energy e on the wave vector \mathbf{k} in the ΓK direction for the graphene with adsorbed potassium impurity [54]

of other computational approaches. However, the realistically typically-experimentally-observed contents of potassium dopant atoms on graphene are substantially smaller ($\geq 0.05-0.1\%$) [57, 58] than those considered in Ref. [54], as well as the sputtered nanoparticles in Refs. [59, 60]. In this context, the smaller potassium concentration has been associated with a smaller band-gap width, as revealed in Refs. [55, 56]. Nevertheless, electronic [55] and diffraction characteristics [61] are sensitive even to a substantially small amount of any disorder (structural imperfections).

10. Summary

The paper reports and analyses a new method of describing the electronic spectrum, thermodynamic potential, and electrical conductivity of disordered crystals based on the Hamiltonian of electrons and phonons. The tight-binding model describes electron states of a system. The Hamiltonian of a system is defined based on the wave functions of electrons in the atomic-nuclei field. Expressions for the Green's functions, thermodynamic potential, and electrical conductivity are derived using the diagram method. Equations are obtained for the vertex parts of the mass operators of the electron-electron and electron-phonon interactions. A set of exact equations is obtained for the spectrum of elementary excitations in a crystal. This makes it possible to perform numerical calculations of the energy spectrum and the properties of a system with a predetermined accuracy. In contrast to other approaches, which account for electron correlations only in the limiting cases of the infinitely large and infinitesimal electron densities, this method describes electron correlations in the general case of an arbitrary electron density. The cluster expansion is obtained for both the density of states and the electrical conductivity of disordered systems. We show that the contribution of the electron-scattering processes on clusters is decreasing along with increasing the number of sites within the cluster that depends on a small parameter.

It is found that a gap appears in the energy spectrum of graphene with an ordered arrangement of potassium atoms. Its value depends on the concentration of adsorbed potassium atoms, their location in the primitive unit cell, and the distance to carbon atoms. It is found that, at such a concentration of potassium that the primitive unit cell includes two carbon atoms and one potassium atom, if the latter is located on the graphene surface above the carbon atom at a distance of 0.286 nm, the band gap is $\approx 0.25 \text{ eV}$.

Acknowledgements. All authors are obliged to the Armed Forces of Ukraine for providing security that made it possible to carry out this work. The paper contains results carried out within the framework of the grants from the Simons Foundation: Awards IDs 1030285 (2023) and 1290592 (2024). The authors acknowledge the National Academy of Sciences of Ukraine for its activity during the martial law and support within the budget departmental researches: 'Multiparametrical phase-variation diagnostics and modelling of electromagnetic properties of structures with inhomogeneously distributed imperfections' (state reg. No. 0123U101504 for 2023–2027) and 'Self-organization of structure, electronic and physical properties of the state-of-the-art metal-containing materials' (state reg. No. 0122U002396 for 2022–2026).

REFERENCES

- 1. W.A. Harrison, Transition-metal pseudopotentials, *Phys. Rev.*, **181**: 1036 (1969); https://doi.org/10.1103/PhysRev.181.1036
- 2. D. Vanderbilt, Soft self-consistent pseudopotentials in a generalized eigenvalue formalism, *Phys. Rev. B*, **41**: 7892 (1985); https://doi.org/10.1103/PhysRevB.41.7892
- 3. K. Laasonen, R. Car, C. Lee, and D. Vanderbilt, Implementation of ultrasoft pseudopotentials in *ab initio* molecular dynamics, *Phys. Rev. B*, **43**: 6796 (1991); https://doi.org/10.1103/PhysRevB.43.6796
- 4. P.E. Blöchl, Projector augmented-wave method, *Phys. Rev. B*, **50**: 17953 (1994); https://doi.org/10.1103/PhysRevB.50.17953
- 5. G. Kresse and D. Joubert, From ultrasoft pseudopotentials to the projector augmented-wave method, *Phys. Rev. B*, **59**: 1758 (1999); https://doi.org/10.1103/PhysRevB.59.1758
- J.P. Perdew, K. Burke, and M. Ernzerhof, Generalized gradient approximation made simple, *Phys. Rev. Lett.*, 77: 3865 (1996); https://doi.org/10.1103/PhysRevLett.77.3865
- 7. J. Tao, J.P. Perdew, V.N. Staroverov, and G.E. Scuseria, Climbing the density functional ladder: nonempirical meta-generalized gradient approximation designed for molecules and solids, *Phys. Rev. Lett.*, 91: 146401 (2003); https://doi.org/10.1103/PhysRevLett.91.146401
- 8. J.P. Perdew, S. Kurth, A. Zupan, and P. Blaha, Accurate density functional with correct formal properties: a step beyond the generalized gradient approximation, *Phys. Rev. Lett.*, 82: 2544 (1999);
 - https://doi.org/10.1103/PhysRevLett.82.2544

- 9. J.P. Perdew, A. Ruzsinszky, G.I. Csonka, L.A. Constantin, and J. Sun, Workhorse semilocal density functional for condensed matter physics and quantum chemistry, *Phys. Rev. Lett.*, **103**: 026403 (2009);
 - https://doi.org/10.1103/PhysRevLett.103.026403
- 10. J. Sun, M. Marsman, G.I. Csonka, A. Ruzsinszky, P. Hao, Y.-S. Kim, G. Kresse, and J.P. Perdew, Self-consistent meta-generalized gradient approximation within the projector-augmented-wave method, *Phys. Rev. B*, 84: 035117 (2011); https://doi.org/10.1103/PhysRevB.84.035117
- V.V. Ivanovskaya, C. Köhler, and G. Seifert, 3d metal nanowires and clusters inside carbon nanotubes: structural, electronic, and magnetic properties, *Phys. Rev.* B, 75: 075410 (2007);
 - https://doi.org/10.1103/PhysRevB.75.075410
- 12. D. Porezag, T. Frauenheim, T. Köhler, G. Seifert, and R. Kascher, Construction of tight-binding-like potentials on the basis of density-functional theory: application to carbon, *Phys. Rev. B*, **51**: 12947 (1995); https://doi.org/10.1103/PhysRevB.51.12947
- 13. M. Elstner, D. Porezag, G. Jungnickel, J. Elsner, and M. Haugk, Self-consistent-charge density-functional tight-binding method for simulations of complex materials properties, *Phys. Rev. B*, **58**: 7260 (1998); https://doi.org/10.1103/PhysRevB.58.7260
- 14. C. Köhler, G. Seifert, U. Gerstmann, M. Elstner, and H. Overhof, Approximate density-functional calculations of spin densities in large molecular systems and complex solids, *Phys. Chem. Chem. Phys.*, 3: 5109 (2001); https://doi.org/10.1039/b105782k
- V.V. Ivanovskaya and G. Seifert, Tubular structures of titanium disulfide TiS₂, Solid State Commun., 130: 175 (2004); https://doi.org/10.1016/j.ssc.2004.02.002
- 16. V.V. Ivanovskaya, T. Heine, S. Gemming, and G. Seifert, Structure, stability and electronic properties of composite Mo_{1-x}Nb_xS₂ nanotubes, *Phys. Status Solidi B*, 243: 1757 (2006);
 - https://doi.org/10.1002/pssb.200541506
- 17. A. Enyaschin, S. Gemming, T. Heine, G. Seifert, and L. Zhechkov, C₂₈ fullerites structure, electronic properties and intercalates, *Phys. Chem. Chem. Phys.*, 8: 3320 (2006);
 - https://doi.org/10.1039/B604737H
- 18. J.C. Slater and G.F. Koster, Simplified LCAO method for the periodic potential problem, *Phys. Rev.*, **94**: 1498 (1954); https://doi.org/10.1103/PhysRev.94.1498
- 19. R.R. Sharma, General expressions for reducing the Slater-Koster linear combination of atomic orbitals integrals to the two-center approximation, *Phys. Rev. B*, 19: 2813 (1979);
 - https://doi.org/10.1103/PhysRevB.19.2813
- 20. L. Bellaiche and D. Vanderbilt, Virtual crystal approximation revisited: Application to dielectric and piezoelectric properties of perovskites, *Phys. Rev. B*, **61**: 7877 (2000);
 - https://doi.org/10.1103/PhysRevB.61.7877
- G.M. Stocks, W.M. Temmerman, and B.L. Gyorffy, Complete solution of the Korringa-Kohn-Rostoker coherent-potential-approximation equations: Cu-Ni Alloys, *Phys. Rev. Lett.*, 41: 339 (1978);
 - https://doi.org/10.1103/PhysRevLett.41.339
- 22. G.M. Stocks and H. Winter, Self-consistent-field-Korringa-Kohn-Rostoker-cohe-

- rent-potential approximation for random alloys, Z. Phys. B, 46: 95 (1982); https://doi.org/10.1007/BF01312713
- 23. D.D. Johnson, D.M. Nicholson, F.J. Pinski, B.L. Gyorffy, and G.M. Stocks, Total-energy and pressure calculations for random substitutional alloys, *Phys. Rev. B*, 41: 9701 (1990);
 - https://doi.org/10.1103/PhysRevB.41.9701
- 24. S. Mu, R.J. Olsen, B. Dutta, L. Lindsay, G.D. Samolyuk, T. Berlijn, E.D. Specht, K. Jin, H. Bei, T. Hickel, B.C. Larson, and G.M. Stocks, Unfolding the complexity of phonon quasi-particle physics in disordered materials, npj Computational Mater., 6: 4 (2020);
 - https://doi.org/10.1038/s41524-020-0271-3
- D. Billington, A.D.N. James, E.I. Harris-Lee, D.A. Lagos, D. O'Neill, N. Tsuda, K. Toyoki, Y. Kotani, T. Nakamura, H. Bei, S. Mu, G.D. Samolyuk, G.M. Stocks, J.A. Duffy, J.W. Taylor, S.R. Giblin, and S.B. Dugdale, Bulk and element-specific magnetism of medium-entropy and high-entropy Cantor-Wu alloys, *Phys. Rev. B*, 102: 174405 (2020);
 - https://doi.org/10.1103/PhysRevB.102.174405
- V.F. Los' and S.P. Repetsky, A theory for the electrical conductivity of an ordered alloy, J. Phys.: Condens. Matter, 6: 1707 (1994); https://doi.org/10.1088/0953-8984/6/9/013
- 27. S.P. Repetsky, I.G. Vyshyvana, S.P. Kruchinin, and S. Bellucci, Influence of the ordering of impurities on the appearance of an energy gap and on the electrical conductance of graphene, *Sci. Rep.*, 8: 9123 (2018); https://doi.org/10.1038/s41598-018-26925-0
- 28. S.P. Repetsky, I.G. Vyshyvana, S.P. Kruchinin, B. Vlahovic, and S. Bellucci, Effect of impurities ordering in the electronic spectrum and conductivity of graphene, *Phys. Lett. A*, **384**, Iss. 19: 126401 (2020); https://doi.org/10.1016/j.physleta.2020.126401
- S. Bellucci, S. Kruchinin, S.P. Repetsky, I.G. Vyshyvana, and R.M. Melnyk, Behavior of the energy spectrum and electric conduction of doped graphene, *Materials*, 13: 1718 (2020); https://doi.org/10.3390/ma13071718
- 30. S.P. Repetsky, I.G. Vyshyvana, S.P. Kruchinin, and S. Bellucci, Theory of electron correlation in disordered crystals, *Materials*, **15**: 739 (2022); https://doi.org/10.3390/ma15030739
- 31. S. Repetsky, I. Vyshyvana, Y. Nakazawa, S. Kruchinin, and S. Bellucci, Electron transport in carbon nanotubes with adsorbed chromium impurities, *Materials*, 12: 524 (2019);
 - https://doi.org/10.3390/ma12030524
- 32. S. Repetsky, I. Vyshyvana, S. Kruchinin, and S. Bellucci, Tight-binding model in the theory of disordered crystals, *Mod. Phys. Lett. B*, 34: 2040065 (2020); https://doi.org/10.1142/S0217984920400655
- 33. S.P. Repetsky and T.D. Shatnii, Thermodynamic potential of a system of electrons and phonons in a disordered alloy, *Theor. Math. Phys.*, **131**, No. 3: 832 (2002); https://doi.org/10.1023/A:1015931708479
- 34. S.P. Repetsky, E.G. Len, and V.V. Lizunov, Electronic structure and spin transport in a Fe-Co alloy, *Metallofiz. Noveishie Tekhnol.*, 28, No. 8: 989 (2006) (in Russian);
 - https://www.researchgate.net/publication/298537053
- 35. S.P. Repetsky, T.S. Len, and V.V. Lizunov, Energy spectrum of electrons and magnetic susceptibility of Fe-Co alloy, *Metallofiz. Noveishie Tekhnol.*, 28, No. 9:

- 1143 (2006) (in Russian);
- https://www.researchgate.net/publication/296795307
- 36. S.P. Repetsky, E.G. Len, and V.V. Lizunov, Electronic structure and magnetic domains in alloys with narrow energy bands, *Metallofiz. Noveishie Tekhnol.*, 28, No. 11: 1471 (2006) (in Russian);
 - https://www.researchgate.net/publication/298574309
- 37. A.A. Abrikosov, L.P. Gor'kov, and I.Ye. Dzyaloshinskii, *Quantum Field Theoretical Methods in Statistical Physics*. 2nd Ed. (Oxford-London: Pergamon Press: 1965); https://www.scribd.com/doc/249903113
- 38. P.O. Löwdin, On the non-orthogonality problem connected with the use of atomic wave functions in the theory of molecules and crystals, *J. Chem. Phys.*, 18: 365 (1950);
 - https://doi.org/10.1063/1.1747632

https://doi.org/10.1007/978-3-319-91083-3 3

- 39. T.M. Radchenko, V.A. Tatarenko, and G. Cuniberti, Effects of external mechanical or magnetic fields and defects on electronic and transport properties of graphene, *Mater. Today: Proc.*, 35, Pt. 4: 523 (2021); https://doi.org/10.1016/j.matpr.2019.10.014
- 40. A.G. Solomenko, R.M. Balabai, T.M. Radchenko, and V.A. Tatarenko, Functionalization of quasi-two-dimensional materials: chemical and strain-induced modifications, *Prog. Phys. Met.*, 23, No. 2: 147 (2022); https://doi.org/10.15407/ufm.23.02.147
- 41. T.M. Radchenko, I.Yu. Sahalianov, V.A. Tatarenko, Yu.I. Prylutskyy, P. Szroeder, M. Kempiński, and W. Kempiński, Strain- and adsorption-dependent electronic states and transport or localization in graphene, Springer Proceedings in Physics: Nanooptics, Nanophotonics, Nanostructures, and Their Applications (Eds. O. Fesenko and L. Yatsenko) (Cham, Switzerland: Springer: 2018), vol. 210, ch. 3, p. 25;
- 42. T.M. Radchenko, I.Yu. Sahalianov, V.A. Tatarenko, Yu.I. Prylutskyy, P. Szroeder, M. Kempiński, and W. Kempiński, The impact of uniaxial strain and defect pattern on magnetoelectronic and transport properties of graphene, *Handbook of Graphene: Growth, Synthesis, and Functionalization* (Eds. E. Celasco and A. Chaika) (Beverly, MA: Scrivener Publishing LLC: 2019), vol. 1, ch. 14, p. 451; https://doi.org/10.1002/9781119468455.ch14
- 43. T.M. Radchenko, V.A. Tatarenko, I.Yu. Sagalianov, and Yu.I. Prylutskyy, Configurations of structural defects in graphene and their effects on its transport properties, *Graphene: Mechanical Properties, Potential Applications and Electrochemical Performance* (Ed. B.T. Edwards) (New York: Nova Science Publishers: 2014), ch. 7, p. 219;
 - https://novapublishers.com/shop/graphene-mechanical-properties-potential-applications- and -electrochemical-performance
- 44. T.M. Radchenko, A.A. Shylau, and I.V. Zozoulenko, Influence of correlated impurities on conductivity of graphene sheets: time-dependent real-space Kubo approach, *Phys. Rev. B*, 86, No. 3: 035418 (2012); https://doi.org/10.1103/PhysRevB.86.035418
- 45. T.M. Radchenko, V.A. Tatarenko, I.Yu. Sagalianov, and Yu.I. Prylutskyy, Effects of nitrogen-doping configurations with vacancies on conductivity in graphene, *Phys. Lett. A*, 378, Nos. 30–31: 2270 (2014); https://doi.org/10.1016/j.physleta.2014.05.022
- 46. I.Yu. Sagalianov, T.M. Radchenko, Yu.I. Prylutskyy, V.A. Tatarenko, and P. Szroeder, Mutual influence of uniaxial tensile strain and point defect pattern on electronic

- states in graphene, Eur. Phys. J. B, 90, No. 6: 112 (2017); https://doi.org/10.1140/epjb/e2017-80091-x
- 47. T.M. Radchenko, V.A. Tatarenko, V.V. Lizunov, V.B. Molodkin, I.E. Golentus, I.Yu. Sahalianov, and Yu.I. Prylutskyy, Defect-pattern-induced fingerprints in the electron density of states of strained graphene layers: diffraction and simulation methods, *Phys. Status Solidi B*, 256, No. 5: 1800406 (2019); https://doi.org/10.1002/pssb.201800406
- 48. P. Szroeder, I. Sahalianov, T. Radchenko, V. Tatarenko, and Yu. Prylutskyy, The strain- and impurity-dependent electron states and catalytic activity of graphene in a static magnetic field, *Optical Mater.*, **96**: 109284 (2019); https://doi.org/10.1016/j.optmat.2019.109284
- 49. D.M.A. Mackenzie, M. Galbiati, X.D. de Cerio, I.Y. Sahalianov, T.M. Radchenko, J. Sun, D. Peca, L. Gammelgaard, B.S. Jessen, J.D. Thomsen, P. Burggild, A. Garcia-Lekue, L. Camilli, and J.M. Caridad, Unraveling the electronic properties of graphene with substitutional oxygen, 2D Materials, 8, No. 4: 045035 (2021); https://doi.org/10.1088/2053-1583/ac28ab
- 50. T.M. Radchenko, A.A. Shylau, I.V. Zozoulenko, and A. Ferreira, Effect of charged line defects on conductivity in graphene: numerical Kubo and analytical Boltzmann approaches, *Phys. Rev. B*, 87, No. 19: 195448 (2013); https://doi.org/10.1103/PhysRevB.87.195448
- I.Yu. Sahalianov, T.M. Radchenko, V.A. Tatarenko, and Yu.I. Prylutskyy, Magnetic field-, strain-, and disorder-induced responses in an energy spectrum of graphene, *Annals of Physics*, 398: 80 (2018); https://doi.org/10.1016/j.aop.2018.09.004
- 52. T.M. Radchenko, A.A. Shylau, and I.V. Zozoulenko, Conductivity of epitaxial and CVD graphene with correlated line defects, *Solid State Commun.*, **195**: 88 (2014); https://doi.org/10.1016/j.ssc.2014.07.012
- 53. I.Yu. Sahalianov, T.M. Radchenko, V.A. Tatarenko, and G. Cuniberti, Sensitivity to strains and defects for manipulating the conductivity of graphene, *EPL*, 132, No. 4: 48002 (2020); https://doi.org/10.1209/0295-5075/132/48002
- 54. S.P. Repetsky, I.G. Vyshyvana, S.P. Kruchinin, V.B. Molodkin, and V.V. Lizunov, Influence of the adsorbed atoms of potassium on an energy spectrum of graphene, *Metallofiz. Noveishie Tekhnol.*, 39, No. 8: 1017 (2017) (in Ukrainian); https://doi.org/10.15407/mfint.39.08.1017
- 55. T.M. Radchenko, V.A. Tatarenko, I.Yu. Sagalianov, Yu.I. Prylutskyy, P. Szroeder, and S. Biniak, On adatomic-configuration-mediated correlation between electrotransport and electrochemical properties of graphene, *Carbon*, **101**: 37 (2016); https://doi.org/10.1016/j.carbon.2016.01.067
- 56. T.M. Radchenko, V.A. Tatarenko, I.Yu. Sagalyanov, and Yu.I. Prylutskyy, Configurational effects in an electrical conductivity of a graphene layer with the distributed adsorbed atoms (K), Nanosistemi, Nanomateriali, Nanotehnologii, 13, No. 2: 201 (2015) (in Ukrainian);
 - https://www.researchgate.net/publication/292463937
- 57. J. Yan and M.S. Fuhrer, Correlated charged impurity scattering in graphene, *Phys. Rev. Lett.*, **107**: 206601 (2011); https://doi.org/10.1103/PhysRevLett.107.206601
- 58. J.-H. Chen, C. Jang, S. Adam, M.S. Fuhrer, E.D. Williams, and M. Ishigami, Charged-impurity scattering in graphene, *Nature Phys.*, 4: 377 (2008); https://doi.org/10.1038/nphys935
- 59. O.V. Khomenko, A.A. Biesiedina, K.P. Khomenko, and R.R. Chernushchenko, Computer modelling of metal nanoparticles adsorbed on graphene, *Prog. Phys.*

- Met., 23, No. 2: 239 (2022); https://doi.org/10.15407/ufm.23.02.239
- 60. O.V. Khomenko, A.A. Biesiedina, K.P. Khomenko, P.E. Trofimenko, and I.A. Chelnokov, Atomistic modelling of frictional anisotropy of metal nanoparticles on graphene, *Prog. Phys. Met.*, 26, No. 2: 219 (2025); https://doi.org/10.15407/ufm.26.02.219
- 61. O.S. Skakunova, S.I. Olikhovskii, T.M. Radchenko, S.V. Lizunova, T.P. Vladimirova, and V.V. Lizunov, X-ray dynamical diffraction by quasi-monolayer graphene, *Sci. Rep.*, 13: 15950 (2023);

https://doi.org/10.1038/s41598-023-43269-6

Received 02.05.2025 Final version 16.08.2025

 $C.\Pi$. Репецький 1,2 , $I.\Gamma$. Вишивана 3 , В.В. Лізунов 1 , P.М. Мельник 2 , M.I. Резников 3 , T.M. Радченко 1 , В.А. Татаренко 1

- ¹ Інститут металофізики ім. Г.В. Курдюмова НАН України, бульв. Академіка Вернадського, 36, 03142 Київ, Україна
- ² Національний університет «Києво-Могилянська академія», вул. Г. Сковороди, 2, 04070 Київ, Україна
- ³ Київський національний університет імені Тараса Шевченка, вул. Володимирська, 60, 01033 Київ, Україна

МЕТОД ГРІНОВИХ ФУНКЦІЙ У ТЕОРІЇ НЕВПОРЯДКОВАНИХ КРИСТАЛІВ: ЗАСТОСУВАННЯ ДО ЛЕГОВАНОГО КАЛІЄМ ГРАФЕНУ

Розглянуто, проаналізовано та розвинуто метод розрахунку енергетичного спектра, вільної енергії й електропровідності невпорядкованих кристалів, що описуються гамільтоніаном електронної та фононної підсистем. Електронні стани системи описано в рамках моделі сильного зв'язку. Запропоновано просту процедуру обчислення матричних елементів гамільтоніана у представленні Ванньє. Вирази для грінових функцій, вільної енергії й електропровідності одержано шляхом використання діаграмної техніки. За допомогою цієї процедури перенормовано вершинні частини масових операторів електрон-електронної й електрон-фононної взаємодій. Одержано систему точних рівнянь для спектра елементарних збуджень кристала. Це уможливило виконання числових розрахунків енергетичного спектра та прогнозування властивостей системи із заданою точністю. Одержано вирази для статичних хвиль концентрацій компонентів, густин заряду та спіну, які визначають фазовий стан невпорядкованого кристала. На відміну від інших підходів щодо опису невпорядкованих кристалічних систем, у яких електронні кореляції враховуються лише в граничних випадках нескінченно великої та нескінченно малої електронної густини, запропонований метод дає можливість описати електронні кореляції в загальному випадку довільної електронної густини. Крім теорії, в статті наведено результати числового розрахунку енергетичного спектра графенового шару з адсорбованими атомами Калію (К). Встановлено, що за концентрації атомів К, коли елементарна комірка містить два атоми Карбону (С) й один атом К, причому останній розташований (адсорбований) на поверхні графенового шару над атомом С на віддалі у 0,286 нм, заборонена енергетична зона становить ≅0,25 еВ. Розташування рівня Фермі (ε_{r}) в енергетичному спектрі залежить від концентрації атомів K і знаходиться в енергетичному інтервалі -0.36 Рід $\leq \varepsilon_F \leq -0.23$ Рід.

Ключові слова: невпорядковані кристали, електронна структура, електропровідність, грінові функції, масовий оператор, густина станів, вільна енергія.